Optical Properties of Snow and Sea Ice

Field Measurements, Parameterization Schemes and Validation

Christina Alsvik Pedersen

A dissertation for the degree of Doctor Scientiarum

UNIVERSITY OF TROMSØ
Faculty of Science
Department of Mathematics and Statistics

December 2007

Abstract

Today we experience an accelerated melting of sea ice in the Arctic which the general circulation models are inadequate to predict. We believe one of the reasons is the shortcomings in the snow and sea-ice albedo schemes for these models. Considering the effect sea ice has on the Arctic climate due to the ice albedo feedback, accurate, physically-based parameterizations schemes for sea-ice albedo are crucial. A new sea-ice albedo parameterization scheme has been developed and implemented in ECHAM5 general circulation model, and includes important components like albedo decay due to snow aging, ice thickness dependency and an explicit treatment of melt pond albedo. Overall, the new albedo scheme reduces the sea-ice albedo, resulting in an overall reduction in sea-ice thickness, concentration and volume, particularly for northern hemisphere in summer due to the inclusion of melt ponds. We have also investigated procedures for collecting and processing datasets describing the sea-ice environment. The focus has varied from small scales (in-situ measurements), regional scales (airborne measurements) and global scales (remote sensing measurements), providing information of the optical properties of snow and sea ice at different resolutions. The small scale measurements were utilized for point-site validation and process studies, while the combinations of airborne measurements provided fractional sea-ice types, sea-ice albedo and sea-ice thickness, thus also estimates for sea-ice area and volume. Such combined datasets are very suitable for validation of climate models. Techniques for appropriate and consistent statistical validation of climate models in general (either to compare climate simulations for different parameterizations, or for validating climate model output against observations) have also been investigated. We have developed an adapted significance-in-scale-space methodology to detect statistical significant differences between two climatological datasets.

Acknowledgments

This PhD study is part of the Norwegian Research Council project "Parameterization of snow and ice albedo in the ECHAM5 General Circulation Model (GCM)". It has been carried out at the Norwegian Polar Institute, and is formally connected to The Department of Mathematic and Statistics at University of Tromsø.

First, I would like to thank my supervisors Jan-Gunnar Winther at Norwegian Polar Institute for all freedom, encouragement and support, and also for making this project possible in the first place, and Fred Godtliebsen at the University in Tromsø for always having time for a discussion or a chat whenever I needed it.

I would like to express my gratitude to the project group; Erich Roeckner at Max Planck Institute for Meteorology, Dorothy K. Hall at NASA Goddard Space Flight Center, Andreas C. Roesch and Atsumu Ohmura at Swiss Federal Institute of Technology, Boris Ivanov at Arctic Antarctic Research Institute and Morten Køltzow at The Norwegian Meteorological Institute. I particularly want to thank Erich for all support and help, and all the time he has spend on the new sea-ice albedo scheme for ECHAM5. I also appreciate all the valuable discussions within the project group at our four project meetings in Hamburg (2002, 2005), Chapel Hill (2003) and Tromsø (2004), and also for the various collaborative works I have had with most of you during this work.

Also, I would like to thank all the people I have been on field excursions with and shared a great time. Glen Liston is acknowledged for making my participation in CLPX field work in Colorado (2003) possible, and Sebastian Gerland is thanked for all field work training, and for being a good and thorough field companion at AIO (2004), Fram Strait Cruise (2005) and in Ny-Ålesund (2007).

I would like to thank my colleagues here at Norwegian Polar Institute and at the University of Tromsø. Particularly, I thank Sebastian and Richard Hall for interesting discussions, Marcel Nicolaus and Jack Kohler for proof-reading and Signe Aaboe for showing me fancy plotting routines in Matlab. The glaciology-lunches every Monday has also been inspiring for my work.

I am very grateful to my family and friends for all support I have received working on this thesis, particularly I want to thank my mum and dad for serving dinners and taking care of Aleksander. I want to thank everybody in Mandagspilsens Venner for fruitful discussions about everything, nothing and even sometimes; physics. Particularly I want to thank Yngvar, Stian, Tor-Arne, Tom-Rune and Rune for answering all my Latex or Matlab questions at various occasions. Last, but certainly not least, I would like to thank my little family; Agnar and Aleksander for the good life we share. During these last busy months, Aleksander always had me thinking about other things than optical properties of snow and ice. Also, Agnar, I am very thankful for all the helpful discussions we have had about my work during this time, and for your never ending support and faith in me.

Contents

1 Introduction

The recent increase in human made greenhouse gases have resulted in a substantial change of the global climate with the average temperature in the Arctic increasing with twice the rate of the global average over the last 100 years (IPCC 4AR; Solomon et al., 2007). Snow, ice-sheets and sea ice used to cover about 15% of the Earth's surface during the peak period in the Northern Hemisphere (March-April), and 6% in August-September (Gerland et al., 2007). But with the increased warming we see substantial decrease in Arctic sea-ice extent (8.9% per decade in September and 2.5% per decade in March, Figure 1.1, IPCC A4R) and sea-ice thickness (Gerland et al., 2007). The snow decrease is not as dominant, since higher temperatures at some temperate locations may imply more snow; however, the mean monthly snow-cover extent in the northern hemisphere has declined with 1.3% per decade over the last four decades, with greatest losses in spring and summer (IPCC AR4).

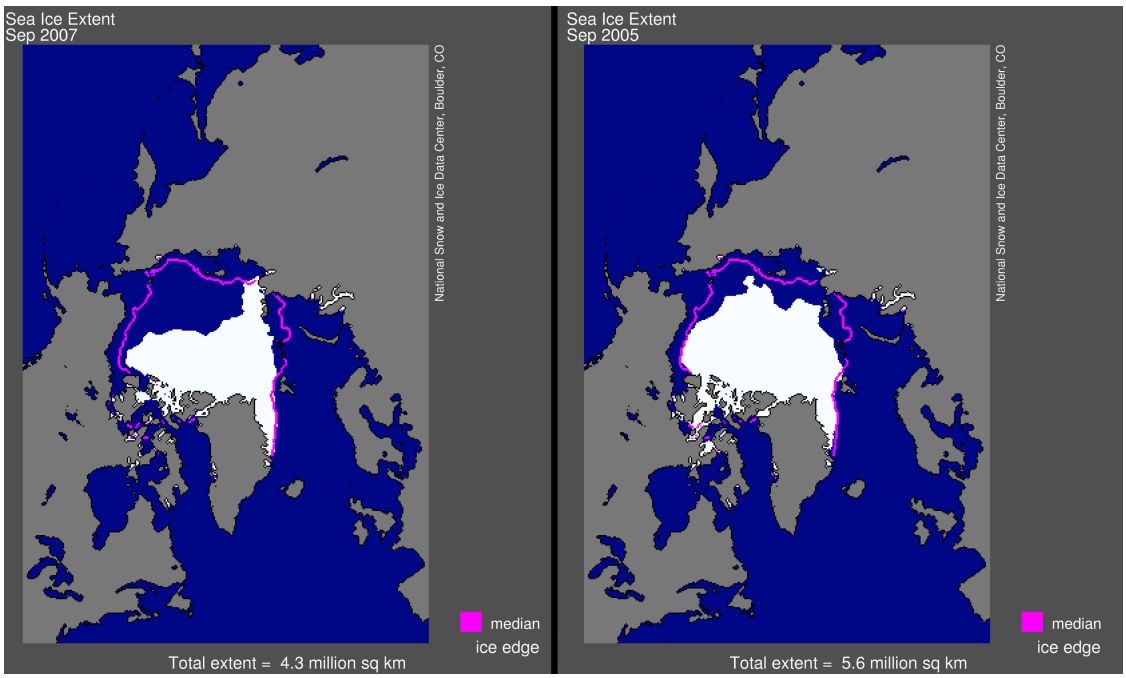

Figure 1.1: Average sea-ice extent for September 2007 ($4.28 \cdot 10^6$ km^2) and 2005 ($5.57 \cdot 10^6$ km^2). The magenta line is the long-term median from 1979-2000. From NSIDC.

Albedo, which is the ratio of reflected to incoming solar radiation at the surface, is one of the most crucial climate parameters. Snow and sea-ice covered surfaces have high albedos, and are particularly sensitive to moderate temperature changes as a warmer climate will expose

surrounding surfaces of substantially lower albedo, *e.g.* tundra vegetation and open water at the expenses of less snow and sea-ice, resulting in most of the sunlight being absorbed, which again leads to further warming. This amplifies warming and creates a positive feedback (Curry et al., 1995; Morassutti, 1991). Before 2050 the ice albedo feedback is projected to accelerate the Arctic sea ice loss substantially (Gerland et al., 2007). These feedback processes, and particularly the sea-ice albedo feedback, are very important for the energy balance in General Circulation Models (GCMs) describing the past, present and future climate. Because of the complexity and difficulties in modeling the sea-ice albedo, up to recently, many GCMs have used the sea-ice albedo as a tuning parameter for realistic sea-ice simulations in the Arctic (Curry et al., 2001). However, as the GCMs and our understanding of the processes involved are improved, the aim is on improving parameterizations for describing the snow and sea-ice albedo.

The main motivation behind this thesis is to create a better and more physically based parameterization for sea-ice albedo to be implemented and tested in ECHAM5 GCM (Roeckner et al., 2003). Both schemes for snow and sea-ice albedo are investigated (Paper I and Appendix A), however we decided to concentrate on the sea-ice albedo because of its strong positive feedback properties, and because of the relative crude parameterizations in the past giving potential for substantial improvements. A new snow albedo parameterization is only included when addressing snow on the sea ice. The thesis also concerns validation of climate models in general, including both measurements for which to validate against, and techniques for performing the validation.

Several important scientific questions are raised during the work with this thesis. These questions are discussed throughout the dissertation, and answers are recapitulated in the concluding remarks.

1. Which parameters affect the optical properties of snow and sea ice, in what ways, and which are important parameters for modeling the snow and sea-ice albedo?

The first two points are addressed in the background information (Chapter 2). The intercomparison and validation of snow albedo schemes from different GCMs are the focus of Paper I. The counterpart for the sea-ice albedo is the focus of Appendix A. The new sea-ice albedo parameterization for ECHAM5, which is the focus of Paper II, separates between snow covered ice, bare ice, melt ponds and open water, and determines the albedo and fraction of each type separately. The most important contribution is the inclusion of melt ponds as a separate stage in the seasonal albedo cycle. To the best of our knowledge, an explicit treatment of melt pond albedo has never been incorporated in GCMs before, and it represents a substantial improvement on the summer sea-ice albedo development. Appendix C discusses how aerosols, and in particular black carbon (soot), affects the optical properties of snow and sea-ice.

2. How does the new and more physically based sea-ice albedo scheme in ECHAM5 modify the climate simulations, particularly for the sea-ice environment?

It is not obvious that a physically more correct parameterization for sea-ice albedo in ECHAM5 improves the overall climate simulations, as all climate parameters interact and depend on each other. As the old albedo scheme are unable to accurately describe *e.g.* the winter snow albedo decay and the development of melt ponds on the sea ice during summer, other processes and parameterizations may indirectly compensate for this. So the new and more physically based albedo scheme may in practice do worse in climate simulations (Eisenman et al., 2007).

However, the goal is to aim for a physically correct parameterizations, and this if further employed in Paper II.

3. How can optical measurements (both *in situ*, airborne and remote sensing) of snow and sea ice be used and combined to describe the Arctic sea-ice environment and provide valuable information for validation purposes?

The validation of a new GCM sea-ice albedo parameterizations scheme requires global, daily datasets of sea-ice parameters (which is the focus of Paper III and Appendix B). Both *in-situ*, airborne and remote sensing measurements of optical properties of snow and ice have been investigated. These measurements differ, to some extent, due to sampling approaches, set ups and footprints, and also due to the techniques used to extract the appropriate information.

4. Which techniques can be used for validating climate models in an appropriate and consistent way?

The physical, or practical, significance is a measure of the physical accuracy of a GCM, and can be determined by an experienced climatologist. However, in order to intercompare GCM schemes or to compare GCM schemes against validation datasets, we propose to use statistical methodologies, which are both consistent, repeatable and not dependent on a skilled climatologist. In Paper IV we investigate possibilities for for such methods, by adapting a significance-in-scale-space methodology for detecting statistical significant differences between GCM model output and validation data.

In short the structure of the thesis is as follows: First, it was identified that it exists significant shortcomings with respect to today's parameterization of snow and sea ice albedo in GCMs (Paper I and Appendix A). Second, since model treatment of sea ice albedo especially lacks a comprehensive physically-based parameterization, and considering the effect sea ice has on the Arctic climate, this has been our focus (Paper II). Third, we have investigated procedures for collecting and processing suitable datasets for albedo validation from airborne measurements (Paper III). Finally, a technique was developed for appropriate and consistent statistical validation of climate models in general (Paper IV).

2 Optical Properties of Snow and Sea Ice

This chapter consists of background information for the four papers in this thesis. It introduce the concepts of electromagnetic radiation, reflection and scattering generally, before focusing on the cryospheric environment (loosely defined as snow and ice) and gives a precise nomenclature of albedo, reflectance and reflectance factor (section 2.1). The main part is dedicated to optical properties of snow and sea, both *in-situ* measurements (section 2.2) and modeling (section 2.3), and the various atmospheric and physical parameters affecting them. Section 2.4 deals with parameterization of snow and sea-ice albedo in climate models, with emphasizes on the ECHAM5 GCM, while section 2.5 introduce the concept of validating climate models in general. The possibilities for remote sensing of optical properties of snow and ice are reviewed in section 2.6, focusing on the Moderate Resolution Imaging Spectroradiometer (MODIS) sensor.

Electromagnetic (EM) radiation can be divided by decreasing wavelengths into radio waves, microwaves, infrared, the visible region (visible light), ultraviolet, X-rays and gamma rays (Figure 2.1). The behavior of EM radiation depends on its wavelength and higher frequencies have shorter wavelengths, and vica versa. The visible (or optical) spectrum is the portion of the EM radiation visible to human eye (emphasized in Figure 2.1). There are no exact bounds to the visible spectrum, but a human eye can react to wavelengths from 400 to 750 nm. Near infrared (NIR) radiation is here used for 750-1400 nm. This study is limited to investigations of the solar radiation part of the spectrum (about 250-4000 nm), however radiation at wavelengths shorter than 300 nm is absorbed in the upper atmosphere and does not reach the Earth's surface. Light is said to have dual nature, and exhibits simultaneously properties of Huygens wave theory and Newtons particle theory (Ohanian, 1989). In the particle description, the energy of electromagnetic waves are quantified, and it consists of discrete packets of energy, called photons. The frequency of the wave is proportional to the magnitude of the particles energy. Photons transport energy as they are emitted and absorbed by charged particles.

2.1 Reflection, refraction and scattering of light

When light interacts with a surface reflection, absorption and scattering may occur. A ray of light is reflected back when it hits a surface, and the angle of incident equals the angel of reflection. Absorption is when the incident light interacts with a medium in such a way that some of the energy is transformed into another form of energy (*e.g.* thermal energy). When light is forced to deviate from its straight trajectory by one or more particles in a medium it passes, scattering occur. The scattering is wavelength dependent, and for particles smaller than the wavelength the scattering is homogeneous. As the particle size increase, the scattering field is more and more inhomogeneous (Bohren and Huffman, 1983). Scattering from

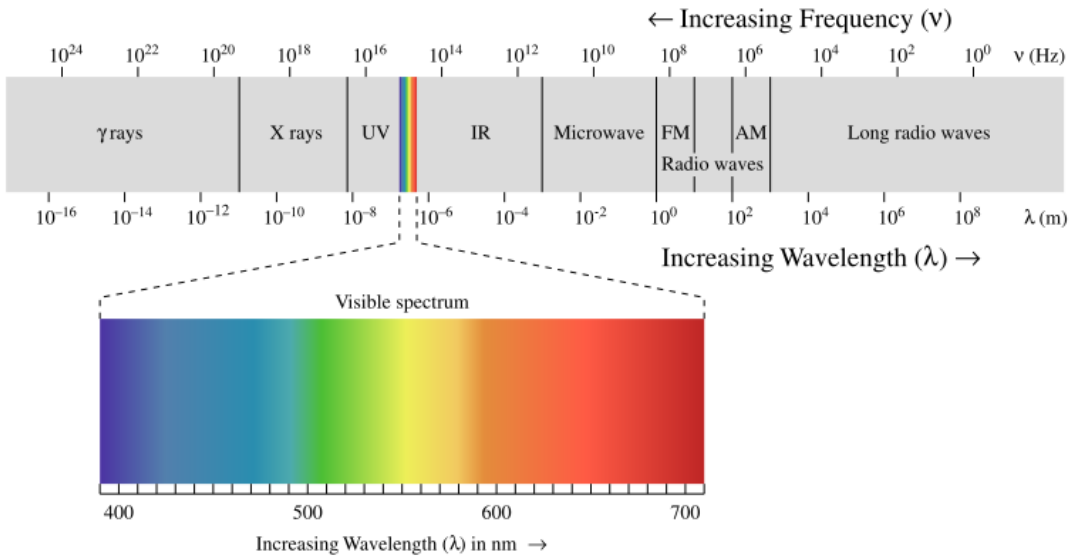

Figure 2.1: The electromagnetic spectrum ranging from radio waves, microwaves, infrared, the visible region, ultraviolet, X-rays and gamma rays for decreasing wavelengths. The visible part of the spectrum ranging from 400 nm (blue) to 700 nm (red) is emphasized. Figure from Wikipedia.

a spherical particle with arbitrary size parameter can be explained by Mie theory, which is a complete analytical solution of Maxwell's equations (Bohren and Huffman, 1983). Rayleigh scattering explains the scattering of light by particles much smaller than the wavelength of the light.

The radiative transfer in sea ice is determined by the absorption and scattering coefficients, brine and impurities. Air bubbles scatter more strongly than brine pockets because of larger differences in refraction index compared to ice. An increasing number of inclusions in sea ice will increase the amount of scattering (Perovich, 2002). Snow has a large number of small grains and ice/air interfaces, which makes it a highly scattering medium, however, particles, like dust or soot in the snow, absorbs light, and threby reduce the scattering. Wiscombe and Warren (1980) (hereinafter WWI) use the Mie theory for single scattering together with the delta Eddington approximation for multiple scattering to describe the reflective properties of snow. More advanced models takes into account the phase function of scattered light, such as the discrete ordinate transform (DISORT) (Stamnes et al., 1988). For more references of the radiative transfer models in snow and ice, see Perovich (2002).

2.1.1 Nomenclature

A common nomenclature for the optical properties of snow and sea ice are required. Irradiance (or flux, F) is the radiant power incident on a unit surface from all directions (unit $\mathrm{W/m^2}$), while radiance I is the radiant power emitted from a unit surface into a unit solid angle (unit $\mathrm{W/m^2/sr^{-1}}$) (Nicodemus et al., 1977). The spectral albedo, which is a function of wavelength,

is given as the ratio of the reflected flux (F_r) to the incident flux (F_i),

$$\alpha(\lambda) = \frac{F_r(\theta_0, \lambda)}{F_i(\theta_0, \lambda)}, \tag{2.1}$$

where θ_0 is the solar zenith angle and λ is the wavelength. $F(\theta_0, \lambda)$ includes both the diffuse and direct (specular) component. The albedo $\alpha(\lambda)$ takes values in the forms $[0, 1]$, or 0-100%. The broadband albedo is obtained by integrating over an arbitrary wavelength interval $\Delta\lambda$

$$\alpha = \frac{\int_{\Delta\lambda} \alpha(\lambda) \cdot F_i(\theta_0, \lambda)\, d\lambda}{\int_{\Delta\lambda} F_i(\theta_0, \lambda)\, d\lambda}, \tag{2.2}$$

while the integrated or total albedo α_{tot} is the spectral albedo integrated over the whole solar spectrum. Changes in the spectral distribution of the incident radiation F_i, caused by *e.g.* changing cloud cover, therefore leads to a changes in broadband and total albedo.

The bidirectional reflectance distribution function (BRDF) is defined as

$$R(\theta_0, \theta, \phi_0, \phi, \lambda) = \frac{I_r(\theta_0, \theta, \phi_0, \phi, \lambda)}{F_i(\theta_0, \lambda)}, \tag{2.3}$$

where I_r is the reflected radiance and the angles $\theta_0, \theta, \phi_0, \phi$, are the solar and sensor, zenith and azimuth angles, respectively. If the surface lacks azimuthally oriented structures, the dependency of ϕ_0 and ϕ can be reduced to the relative azimuth angle $\phi' = \phi_0 - \phi$ (Figure 2.2). The spectral reflectance is the BRDF from nadir (zenith, $\theta = 0°$) direction, while the spectral reflectance factor is defined as the ratio of the radiance reflected by the surface to what would be reflected into the same beam-geometry by an ideal perfectly diffuse (Lambertian) standard surface. In field a Spectralon surface can be used, which reflects 99% of the solar irradiance at 400-1500 nm (Labsphere, 2007). Consequently, the nadir spectral reflectance factor is always higher than the nadir spectral reflectance. (In Figure 2.5 field measurements of spectral albedo and spectral reflectance factor for the same surfaces are intercompared.)

The radiation reflected by a snow cover consists of a specular (direct) component in accordance with optical geometry and a volume (diffuse) component according to Lamberts Law. The specular component is sensitive to the angle of incident light, while the volume component depends on the scattering and absorption properties of the snow. The effect of clouds is to increase the diffuse fraction. Under overcast conditions snow acts as a Lambertian reflector. Often the terms directional-hemispherical reflectance, $\bar{\alpha}(\theta_0)$, or black-sky albedo, is used for the direct part of the albedo, while bi-hemispherical reflectance, $\bar{\bar{\alpha}}$, or white-sky albedo, is used for the diffuse part. The albedo can then be calculated if the diffuse part of the illumination, D, is known, as

$$\alpha = (1 - D)\bar{\alpha}(\theta_0) + D\bar{\bar{\alpha}} \tag{2.4}$$

2.2 In-situ measurements

Numerous papers present the spectral albedo and reflectance of snow and sea ice. Surface reflectance and albedo at Svalbard have been investigated by Gerland et al. (2004, 1999a,b); Winther et al. (1999), and trends calculated by Winther et al. (2002). Perovich and coworkers have examined the optical properties of sea ice (Grenfell and Perovich, 2004; Perovich et al., 2002a,b, 1998; Perovich, 1998, 1994a,b; Grenfell and Perovich, 1984) for different surface characteristics, sites and seasons. Morassutti and Le Drew (1996) collected over 500

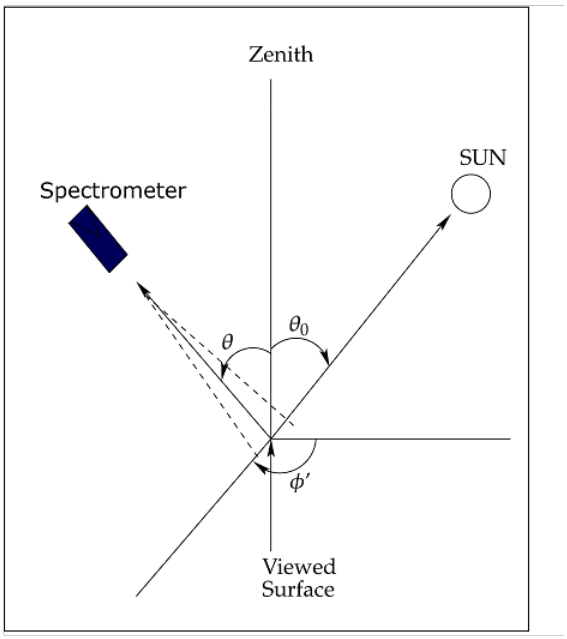

Figure 2.2: Sun-surface-spectrometer geometry, where θ_0 is the solar zenith angle, and θ is the view zenith angle. If the surface lacks azimuthally oriented structures the dependency of the azimuth angles can be reduced to a relative azimuth angle ϕ' (the difference between the solar and view azimuth angles). Here, the view azimuthal angle is defined relative to the solar principal plane.

measurements of melt pond albedo and its properties in the Canadian Arctic. Spectral albedo measurements were made over numerous first year sea-ice surfaces during melt in the Canadian Arctic Ocean (Hanesiak et al., 2001), over first-year sea ice in the Arctic Basin (Grenfell and Maykut, 1977), and in the coastal fast ice in the Gulf of Finland (Rasmus et al., 2002), just to mention a few.

Fresh snow looks white to the human eye because it is highly reflective with little variations over the visible part of the spectrum. A similar argument holds for dark open water, which looks black since it is highly absorptive and relative constant (0.06-0.07) in the visible. The albedo of snow and sea ice is influenced by the surface characteristics and the atmospheric conditions (including the solar zenith angle and cloud conditions). Snow and ice have similar optical properties in the visible and near-IR wavelengths, so albedo in these wavelengths depends primarily on variations in the refractive index of ice and snow. Ice is very weakly absorptive in the visible (minimum absorption at 460 nm), but has strong absorptive bands in the near-IR. The near-IR albedo of snow is very sensitive to snow grain size and moderately sensitive to solar zenith angle. The visible albedo is mostly affected by snow pack thickness and impurities.

2.2.1 Total albedo and seasonal albedo evolution

The total albedo for various sea-ice surfaces from Perovich et al. (1998) are given in Figure 2.3. New snow has the highest total albedo, and when the snow age the albedo is reduced. Frozen ice has higher albedo than melting ice, and the albedo decrease for thinner ice and for melt water on the ice. Open water has the lowest total albedo. A typical time series of total albedo

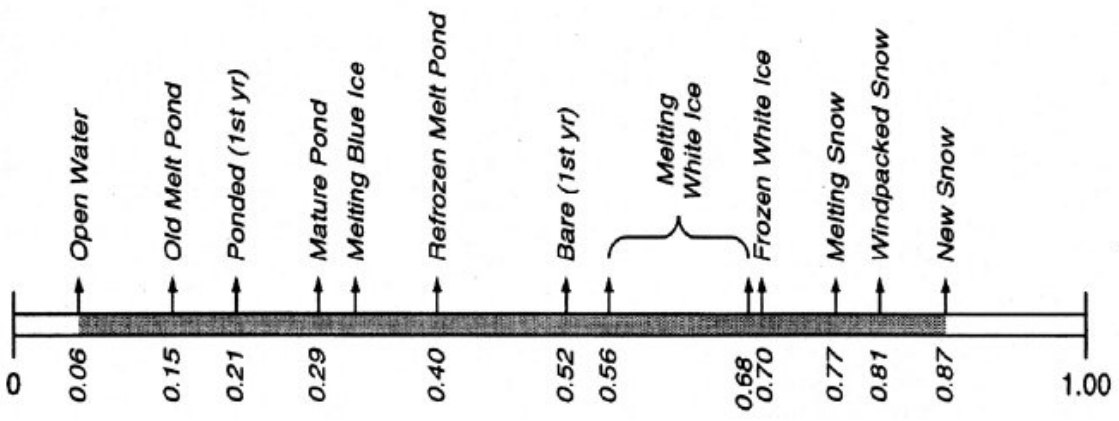

Figure 2.3: Total albedo for different snow and sea-ice covered surfaces, ranging from open water albedo at 0.06 to new, dry snow albedo at 0.87. From Perovich et al. (1998).

from the Surface Heat Budget of the Arctic Ocean (SHEBA) site during one melt season in 1998, after Perovich et al. (2002a), is shown in Figure 2.4b. The albedo was measured every few meters and the total albedo values were averaged over the 200 m "albedo-line". As the figure indicate the seasonal evolution of sea-ice albedo can be divided into five distinct phases; dry snow, melting snow, pond formation, pond evolution and fall freeze-up. During the first phase in winter and early spring the sea ice is covered with a relative thick, homogeneous snow cover, and the total albedo is high reaching values of 0.8-0.9. As the snow gets older and warmer the snow grain size increases and the albedo gradually decreases. Rain often initiates the second phase where the albedo drops substantially, and initiate higher spatial variability. The third phase initiates melt pond formation and reductions in albedo as the melt ponds grow deeper and cover larger areas. At the end of this phase the spatial variability is largest. When the surface temperatures falls below freezing, a light snowfall will increase the albedo substantially. Eventually, when the snow gets deeper during fall the albedo returns to its maxima spring values and is again spatially uniform (Perovich et al., 2002a).

2.2.2 Spectral albedo

Typical spectral albedo measurements of snow show high values in the near-UV and visible part of the spectrum and drops with wavelengths (see Figure 2.4b for examples). The snow albedo varies little in the visible, giving the snow a white appearance, however, a weak maxima can be found at blue and green wavelengths. Spectral albedo measurements of clean, new and dry snow can in the visible reach values up to 0.95-0.98 (Grenfell et al., 1994; Perovich, 1994a). The peaks and valleys of the spectral albedo of snow in the near-IR coincide with the minima

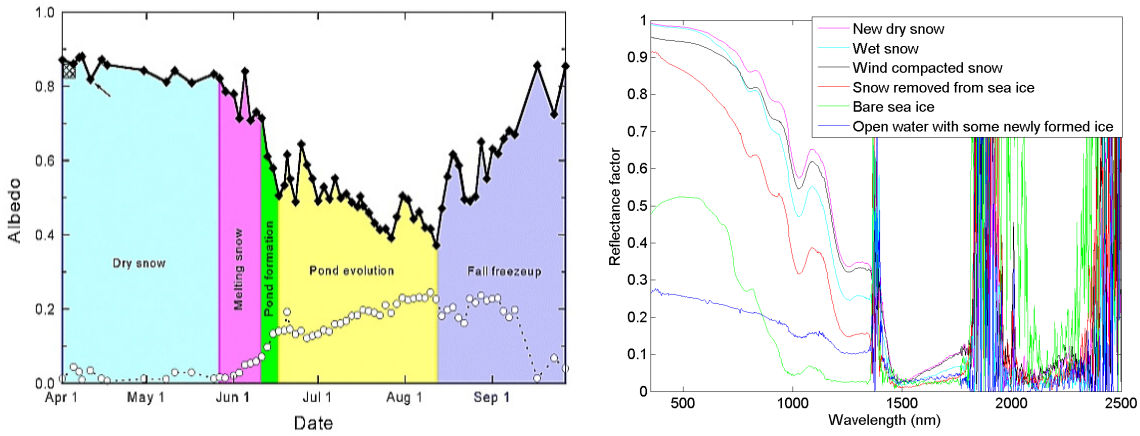

(a) (b)

Figure 2.4: (a) Time series of total albedo at SHEBA site (April-September 1998). The open circles show the standard deviation. From Perovich et al. (2002a). (b) Spectral reflectance factor measurements as a function of wavelengths for typical sea-ice surfaces from Fram Strait in spring 2005. The noisy measurements at some longer wavelengths are due to low signal-to-noise ratio.

and maxima, respectively, of the absorption coefficient of ice. Ice is weakly absorptive in the visible, with local minima of the absorption coefficient of ice at 1100, 1300, 1800 and 2200 nm (WWI). When the snow ages or melts, the grain size increases, and the spectral albedo is reduced at all wavelengths (this will be further discussed in section 2.3.2).

The spectral albedo of open water is about 0.07 and independent of wavelength (Brandt et al., 2005). When thin ice first starts to form on the ocean, only a slight increase in albedo is observed, but as the ice thickens more, the albedo increase at all wavelengths, but most rapidly between 400-500 nm, giving the ice a blue-green appearance. There is a sharp decrease in albedo due to ponding of the ice. The spectral variations for melt ponds are pronounced, with a narrow peak at blue-green wavelengths (Perovich, 1994a). Air bubbles in the ice increase the albedo for all visible and near-IR wavelengths (Perovich, 1994a). A thin snow cover on the ice causes a dramatic increase in albedo, particularly in the near-IR (Brandt et al., 2005).

The general shape of the spectral albedo and reflectance factor are similar for the different snow and sea-ice types. Spectral albedo and spectral reflectance factor for the same surfaces were intercompared by Perovich (1998, 1994a) (Figure 2.5). For snow, the nadir reflectance factor is slightly higher than the albedo, with the deviations constant with wavelengths (Perovich, 1994a). For all the other surfaces, the difference between albedo and reflectance factor is largest in the visible and decreases with increasing wavelengths. The largest difference in the visible (0.1-0.15) is for glazed ice, where the reflectance factor is much larger than the albedo because of the strong forward reflection component. For melt pond the difference between albedo and reflectance factor is largest at longer wavelengths, and the factor between the two (anisotropic reflectance factor) is only 0.25 at 1000 nm. The nadir reflectance spectra in Figure 2.5d are similar in shape, but shifted in magnitude compared to the corresponding spectral albedos in Figure 2.5c (Perovich, 1998). The nadir reflectance is larger than albedo

for dry snow, but is less for the other surfaces, and the anisotropic reflectance factor is largest for the two snow surfaces and melt ponds. The results above emphasize the importance of using a precise terminology.

2.2.3 Practical Considerations

Spectral albedo, reflectance and reflectance factor can be measured with spectrometers. Modern spectrometers cover broad wavelength ranges, have high spectral resolution and are fast. The ASD Field Spec Pro Spectrometer I have used for our measurements cover the wavelength 350-2500 nm and have resolution down to one nm. For the irradiance spectra and spectral albedo measurements a hemispherical and integrating sphere cosine collector is used in front of the detector. The detector is mounted on a long arm (1-2 meters long) to minimize shadowing from the set-up on the surface, and the arm is mounted on a tripod for easy and accurate leveling. For reflectance and reflectance factor measurements, a restricted field-of-view fore-optics is mounted in front of the detector, giving a radius of the field-of-view circle equal to $\tan\frac{\theta}{2} \cdot h$, where h is the hight from the ground (typically about 75 cm), and θ is the field-of-view angle. The largest uncertainty in the spectral albedo measurements occur when the incident irradiance is very low, due to a low signal to noise ratio at these wavelengths particular at 1400 and 1900 nm and above 2300 nm (see Figure 2.4b for examples).

When measuring spectral albedo, reflectance and reflectance factor *in-situ* a few aspects are important and should be considered: (i) Attention on what is measured; Spectral albedo, BRDF, spectral reflectance or spectral reflectance factor are different measures of the optical properties of snow and sea ice (section 2.1.1). (ii) The different measurements have different foot-prints, consequently the surface area actually seen by the instrument vary in size from a few cm^2 to a few m^2. (iii) Light conditions; When measuring albedo with the ASD Field Spec Pro Spectrometer, the sensor needs to be turned, adjusted and leveled between each up and down measurements. Variable light conditions caused by a scattered cloud cover will affect the individual measurements, and give erroneous albedo measurements. (iv) A variable cloud cover makes it difficult to intercompare measurements taken at different times over different surfaces as the cloud cover affects the composition of direct and diffuse radiation, and hence the optical measurements (more in section 2.3.1). (v) The set-up of the instrument requires throughly thoughts: The tripod and arm for measuring albedo can cast shadow the ground, which will affect the albedo measurements. These shadow effects should be avoided or corrected for.

2.3 Optical properties from radiative transfer models

The natural variability of snow and sea-ice albedo due to atmospheric factors (cloud cover, solar angle) and snow and ice physical properties is large. Considerable efforts have been made in understanding the optical properties of snow. WWI and a similar work including aerosols by the same authors (Warren and Wiscombe, 1980) calculate the snow albedo at any wavelength as a function of solar zenith angle, snow grain size, snow thickness, the ratio of diffuse to direct radiation and impurities. Grenfell (1983) presents a radiative transfer model for optical properties of sea ice as a function of ice salinity, temperature, initial growth rate and density of the ice. In the next sections radiative transfer models (primarily from WWI) are used for describing the spectral albedo dependencies from the atmospheric, and snow and sea-ice physical properties.

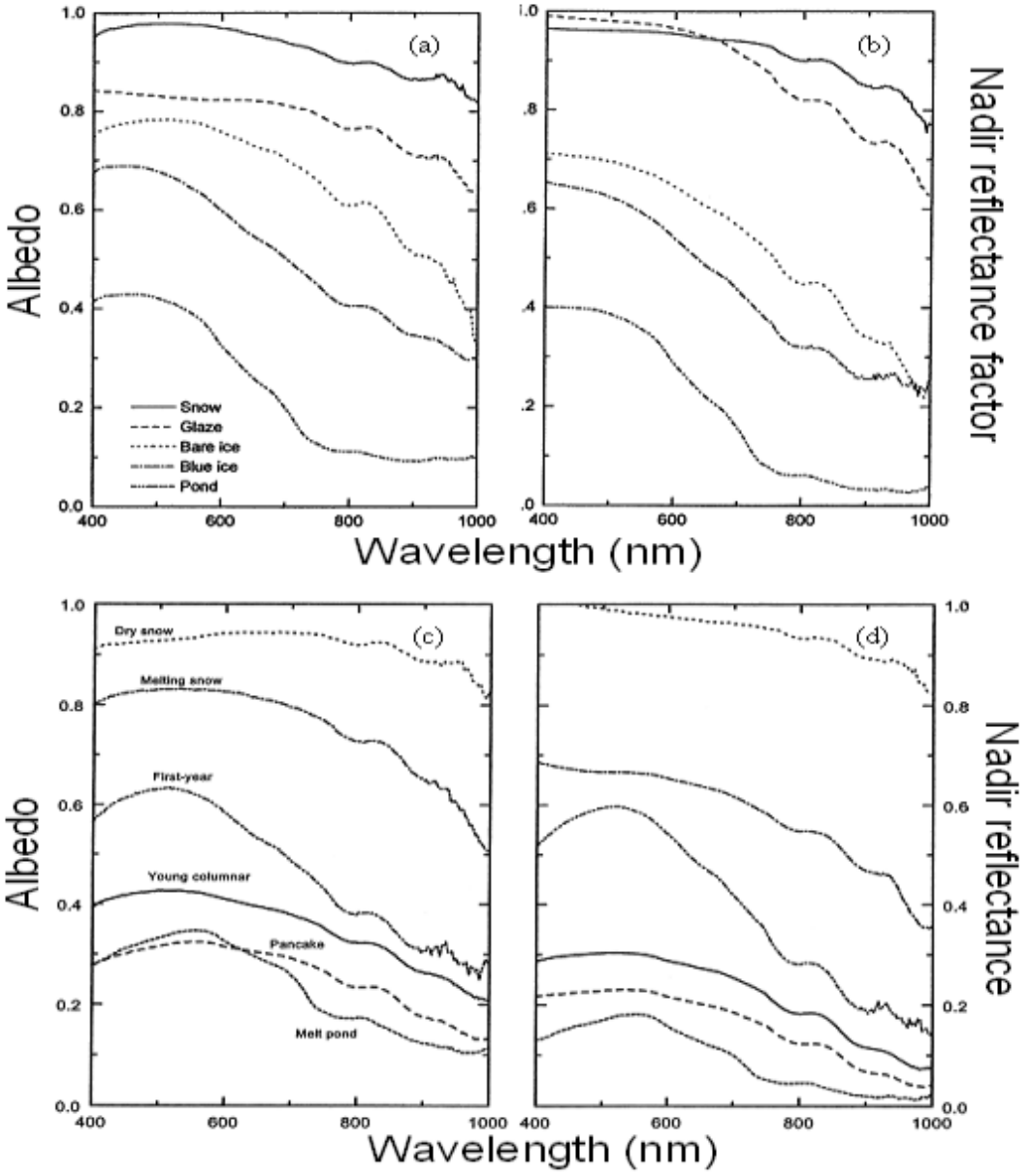

Figure 2.5: Spectral albedo and spectral reflectance/reflectance factor as a function of wavelength for different snow and sea-ice surfaces. (a) Spectral albedo and (b) nadir reflectance factor for snow covered ice, glazed snow over ice, bare ice, blue ice and ponded ice. From Perovich (1994a). (c) Spectral albedo and (d) nadir reflectance for dry snow, melting snow, first year ice, young columnar ice, pancake ice and melt pond. From Perovich (1998).

2.3.1 Effects from the Sun angle and clouds

The albedo of snow increases as the Sun zenith angle increases (low solar elevation) particularly in the near-IR. Relative to a Sun at zenith, the albedo increases only a few percent in the visible, but by as much as 0.2 in the near-IR (WWI). The changes are most rapid for large zenith angles, as it is dependent on the cosine of the zenith angle (Figure 2.6a). As an empirical rule-of-thumb snow albedo is virtually independent of solar zenith angles below 50°. The albedo is higher for lower Sun elevation because on average a photon undergoes its first scattering closer to the surface if it enters the snow pack at a large zenith angle. If the photon is sent in an upward direction its chance of escaping without being absorbed is greater.

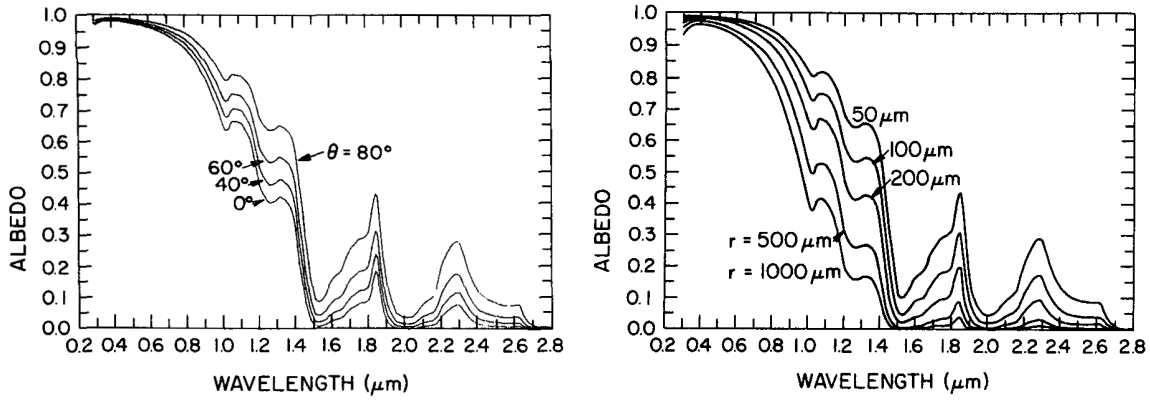

(a) (b)

Figure 2.6: (a) Modeled direct albedo as a function of wavelength for different zenith angles. (b) Modeled direct albedo as a function of wavelengths for various grain radius. From WWI.

Clouds have the effect of diffusing the incoming solar radiation, *i.e.* to change the effective zenith angle (Figure 2.7). The effective zenith angle for purely diffuse radiation is about 50° (Warren, 1982). Thus, a cloud layer between the Sun and the surface cause the spectral albedo to increase for zenith angles smaller than 50° and to decrease for zenith angles greater than 50°, with the first as the most common situation. The integrated snow albedo increases with increasing amounts of clouds as the clouds are non-absorbing at visible wavelengths emphasizing the high visible snow albedo compared to the low near-IR snow albedo. Albedo measurements carried out under diffuse solar radiation penetrates deeper in the snow pack compared to under direct radiation for relatively large zenith angles at 60-70° (Gerland et al., 2000), which affects the albedo, particularly for shallow snow packs.

2.3.2 Snow

During the cold winter months the snow forms a homogeneous thick layer with relative stable and high total albedo (*e.g.* Figure 2.4a). As the snow ages, the albedo decreases, and in spring the snow melt giving a patchy and heterogeneous snow cover with relatively lower albedo.

Snow depth

The albedo of a thin snow cover obviously depends upon the albedo of the underlying surface, and only when the snow becomes thick enough ("optically thick") the effects of the underlying

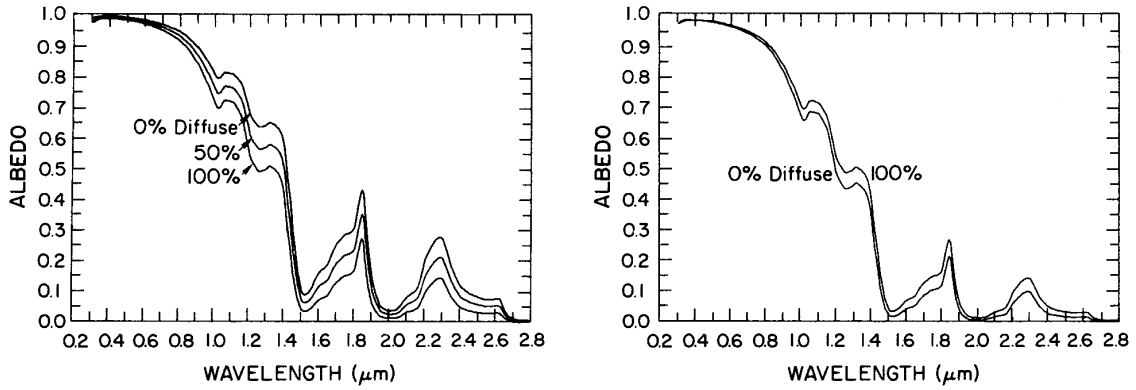

(a) (b)

Figure 2.7: Modeled albedo as a function of wavelengths and various ratio of diffuse to direct radiation for solar zenith angle of 80° in (a), and 30° in (b). From WWI.

surface can be ignored. The thickness threshold for an optical thick snow pack depends primarily on the grain size, as well as the wavelength (Figure 2.8). For longer wavelengths only a thin snow cover is required to make the snow pack optically thick (WWI). For the visible, a snow cover of approximately 20 cm of new fluffy snow (with grain size of 50 μm), 20 cm of fine-grained old snow (with grain size of 200 μm) or 50 cm of old snow (with grain size of 1000 μm) gives an albedo within 1% of the albedo for a very deep snow pack (WWI), consequently the snow is more transparent after the onset of melt (Gerland et al., 2000). Other studies showed that substantially shallower snow depths are required to mask the underlying surface, *e.g.* a snow depth of 5 cm were required to completely cover the underlying soil surface (in terms of total albedo) in Baker et al. (1991), while Brandt et al. (2005) used 3 cm as a threshold for "thick" snow.

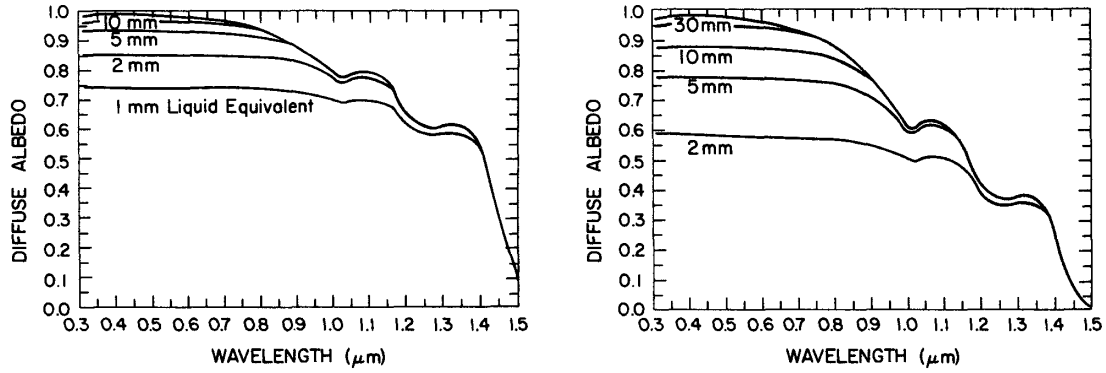

(a) (b)

Figure 2.8: Diffuse spectral albedo as a function of wavelengths for different snow depths and grain radii. A grain radius of 50μm is used in (a) and 200μm in (b). The top curve in each plot is for semi-infinite depths. From WWI.

Grain size

The snow albedo drops at all wavelengths as the grain size increases. The effect is most dominant around 1000 nm and to a lesser extent at shorter and longer wavelengths. The albedo is proportional to the square root of the spherically grain size radius (Bohren and Barkstrom, 1974; Warren, 1982) (Figure 2.6b). The optical grain size of snow increases with age, and generally varies between 50μm for new snow and 1 mm for old melting snow (Warren, 1982). However, the optical grain size is not equivalent to the physical grain size (observed *in-situ*) and generally the snow grains are not spherically. Usually the optically equivalent sphere is assumed to have the same volume to surface ratio as the non-spherical snow crystal observed in the field (WWI; Massom et al., 2001). The physical average grain size radius vary between 20-100 μm for new snow, 100-300 μm for fine-grained older snow, 1.0-1.5 mm for old snow near the melting point (WWI) and above 5 mm for depth hoar. The albedo decreases at longer wavelengths as the grain size increase, because a photon has a chance to be scattered when it crosses an air-ice interface and to be absorbed only when passing through ice. An increase in grain size, causes an increase in the path length to be traveled through ice between scattering opportunities.

Snow density does not directly affect the optical properties of snow, but as the grain size normally increases when the density increases, a decrease in snow albedo can be observed. The density of new snow increases rapidly (termed metamorphism) with changes in the snow pack characteristics caused by temperature and water vapor gradients, crystal settlements and wind packing (Pomeroy and Gray, 1995). The average snow pack density varies seasonally from 100 kg/m^3 for new snow, with increased density in spring and melting snow density commonly in the range 350-500 kg/m^3 (Pomeroy and Gray, 1995). The presence of liquid water (snow water equivalent, SWE) in the snow pack has little direct effect of the albedo, but similar as the density, it has an indirect effect where increasing SWE promotes clustering of the snow crystals leading to larger effective grain size (WWI; Rees, 2006) .

Impurities

Inorganic impurities like black carbon (soot), mineral dust and volcanic ash lower the albedo of snow in the visible even in relative small amounts as they absorb the radiation. In the near-IR, impurities have virtually no effect. Black carbon lowers the albedo substantially more than dust and ash, and approximately 100 ng of impurities per g for snow (ng/g) of black carbon or 10 000 ng/g of desert dust reduce the visible snow albedo by a few percent (Warren and Wiscombe, 1980) (Figure 2.9a). Black carbon are about twice as effective in lowering snow albedo if the soot particles are dispersed inside snow or ice grains, rather than forming an external mixture of soot particles and snow/ice grains (Warren and Wiscombe, 1980). A recent experiment showed total surface albedo to be exponential dependent on the black carbon amount from a local source (Bøggild et al., 2006). Black carbon in snow has strong climate forcings with an efficasy more than three times greater than forcings by CO_2 (Flanner et al., 2007). This topic is further investigated in Appendix C.

2.3.3 Sea ice

The albedo of sea ice depends primarily on the sea-ice type (and consequently the sea-ice thickness) and surface conditions, such as ice crust and frost flowers on the ice (Perovich, 1994b; Barry, 1996). Secondary effects include brine and air bubbles in the ice. During the

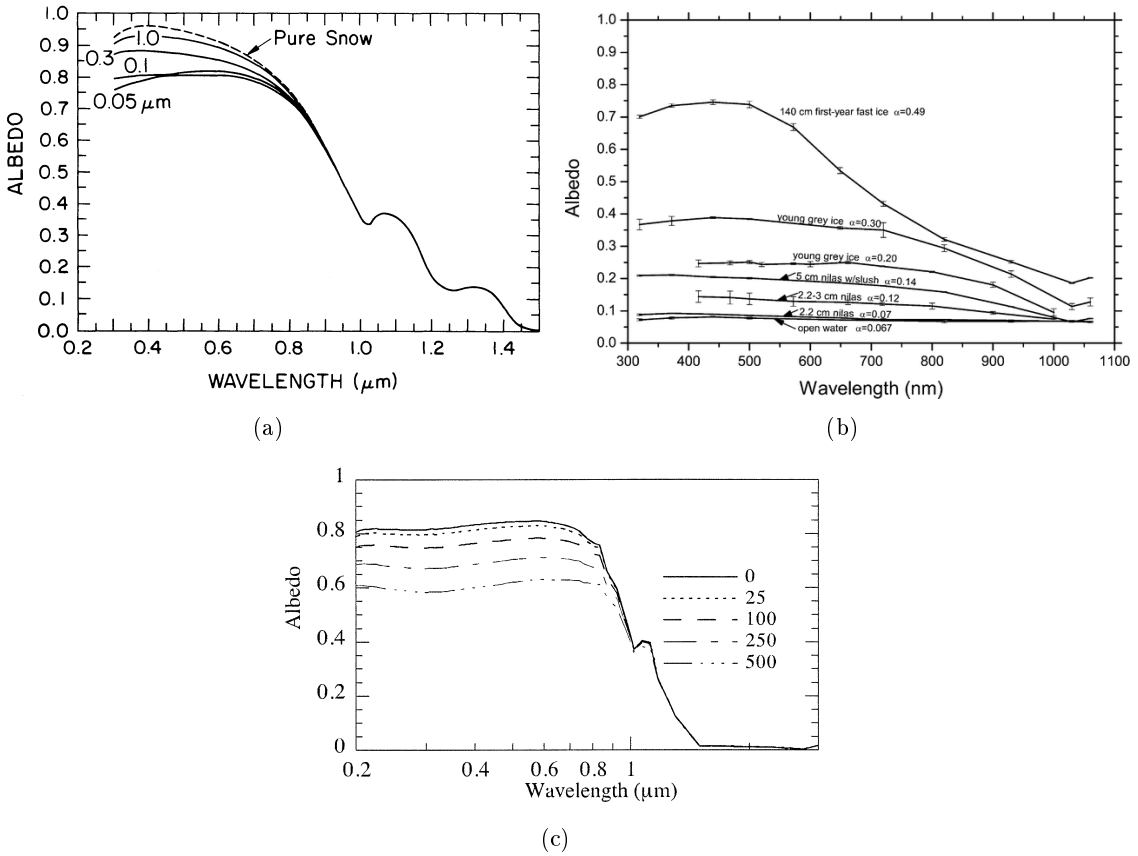

Figure 2.9: (a) Modeled direct beam snow albedo as a function of wavelengths for various sizes of black carbon with concentration 300 ng/g. From (Warren and Wiscombe, 1980). (b) Spectral albedo as a function of wavelengths and total albedo for different sea-ice types and thicknesses. From Brandt et al. (2005). (c) Modeled spectral albedo of sea ice as a function of wavelength for different BC concentrations. From Jacobsen (2004)

melt season, the presence of melt ponds on the ice substantially lower the albedo. The area average total sea-ice albedo certainly depend on the sea-ice fraction, *i.e.* the distribution of open water, leads and polynias.

Sea-ice types

The sea-ice can be divided in new ice, first year ice and multi year ice. New ice is the general term for recently formed ice composed of ice crystals which are only weakly frozen together or not frozen together at all. It includes (Secretary of World Meteorological Organization, 1970) **frazil ice**, which is a collection of randomly oriented needle-shaped ice crystals in water, which at a later stage turn into **grease ice** where the crystals have congulated to form a oily layer at the surface, which gives the water surface a mat and greyish appearance that reflects little light. At a later stage, grease ice forms a thicker continuous and transparent sheet of **young ice (nilas)**. As the ice grows thicker the nilas takes on a grey and finally a white appearance. Waves and wind act to compress the ice particles into larger plates called

pancake ice. Pancake ice can be several meters in diameter and float on the ocean surface colliding with one another to form upturned edges. The pancake ice may be rafted over one another or frozen together into a more solid ice cover with a rough appearance on top and bottom. The albedo and the relation to thickness types are further discussed in Paper III. First year ice is formed in the winter and melts the next summer, while multi year ice has survived at least one summer. The term second year ice is also sometimes used. When the ice gets older, it tends to become thicker, fresher and rougher. Arctic sea-ice cover is mostly composed of thick multi-year ice of a few meters, with an average snow cover depth of 40 cm (Warren et al., 1999).

The albedo of sea ice is primarily determined by the sea-ice type (Brandt et al., 2005, T. Grenfell, perosnal communication) (Figure 2.9b). The albedo of open water is 0.07 relatively independent of wavelengths. The albedo of a 2-cm nilas is almost indistinguishable from that of water, only with a slight increase in the visible. The albedo increase at all wavelengths as the ice thickens (Brandt et al., 2005). The sea ice exhibit large spatial variability, and over small areas open water, thin, young ice and pressure ridges of several meters thickness can be observed. In winter snow covers the sea ice. The snow drifts with the wind, and the depths can vary from zero on bare ice to more than a meter. In summer, melt ponds form.

Snow cover

If the sea ice is snow covered, the albedo is almost completely determined by the snow cover, depending on the thickness of the snow (WWI). The situation is similar to the snow albedo dependency on snow thickness, except the underlying surface is bare ice, not soil (see Figure 2.8). Brandt et al. (2005) provides total albedo for several sea-ice types without snow, with thin snow ($<$3 cm) and with thick snow ($>$3 cm), *e.g.* the average visible albedo increased from 0.67 for bare thick first year ice via 0.92 for the same surface with a thin snow cover to 0.94 with a thick snow cover. Measurements indicate that even as little as 1 cm of snow should be defined as thick ice for the purpose of albedo, however, snow with thicknesses less than 3 cm tends to be patchy (Brandt et al., 2005). The thickness of the snow forming on the sea ice is affected by the sea-ice morphology, particularly ridges, and the snow tends to pile up at certain locations. Snow dunes, or sastrugies, is the result of blowing wind, which can create shadows at the surface and modify the angular reflectance at high zenith angles.

Ice thickness

The sea-ice types from above partly corresponds to sea-ice thickness classes and consequencely determines the albedo (Figure 2.9b). The albedo of snow free sea ice increases with ice thickness up to a certain threshold (about 80 cm with a slight wavelength dependency) where the ice is optically thick (Rasmus et al., 2002), and a further increase in thickness does not affect the albedo.

Ice physical parameters

On smaller scales, brine volume, density of air bubbles and the amount of melt water in the ice affects the radiative scattering in the ice, and consequently the albedo. The brines are the major contributor to volume scattering, with vapor bubbles as a second contributor (Grenfell, 1983). The density of ice affects the albedo, and bubble free dense ice has lower albedo than less dense ice in the visible and near-IR with maximum difference at green wavelengths

(Figure 2.10a). Changes of growth rate of one order of magnitude change the albedo with 20-30% (Figure 2.10b).

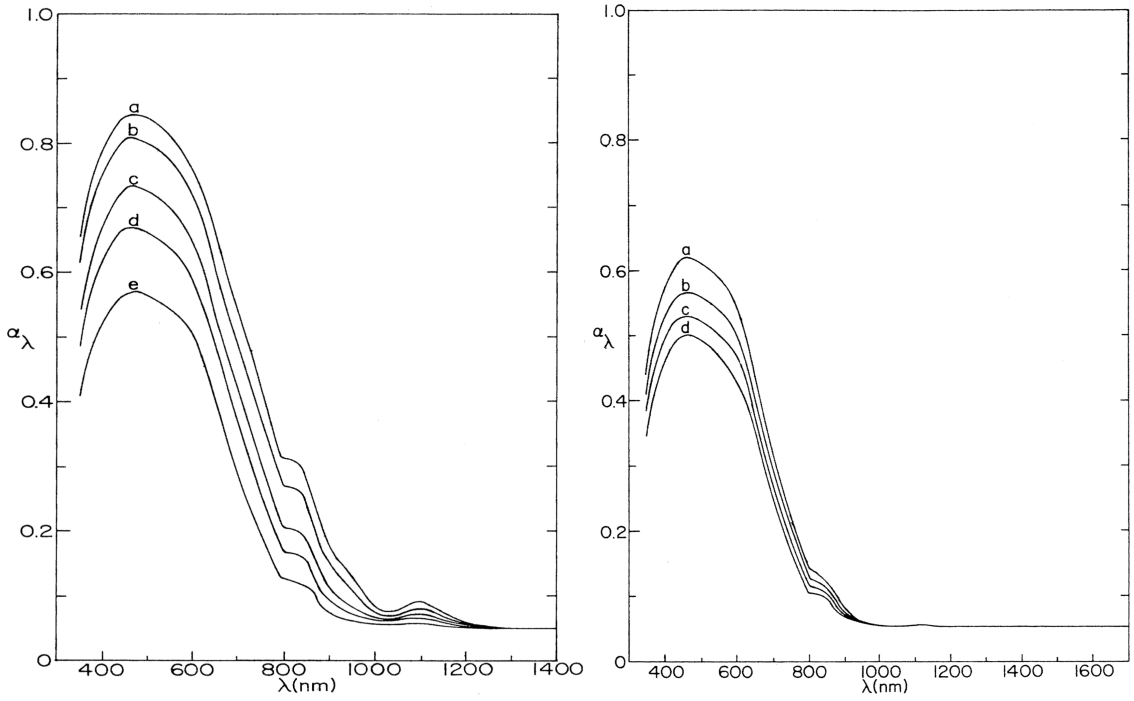

(a) (b)

Figure 2.10: Modeled spectral albedo of sea ice as a function of wavelengths from a radiative transfer model (Grenfell, 1983). (a) Spectral ice albedo for different ice densities; a: 860 kg/m^3; b: 880 kg/m^3; c: 900 kg/m^3; d: 910 kg/m^3; e: 940 kg/m^3 (bubble free ice). (b) Spectral ice albedo for different ice growth rates at; a: 8×10^{-7} m/s; b: 4×10^{-7} m/s; c: 2×10^{-7} m/s; d: 8×10^{-8} m/s. From Grenfell (1983).

Impurities

The effect of black carbon on sea ice is of the same magnitude, but slightly less, compared to snow. 25 ng/g of black carbon reduce the sea-ice albedo at 550 nm by 2.1% (Figure 2.9c), when every snow grain contains a internally mixed black carbon particle, and the rest is assumed to the externally mixed (Jacobsen, 2004).

2.4 Albedo schemes in climate models

One of the key components driving the climate is energy absorbed at the surface, and sensitivity for surface albedo is directly or indirectly incorporated into all General Circulation Models (GCMs). GCMs predict temperature changes associated with global warming to be largest at high latitudes, predominantly due to positive feedbacks. The snow-albedo feedback, which generates from a reduced snow extent and decrease in wintertime land surface albedo, would accompany a warmer climate because of increased absorbed radiation. This again leads

to reduced snow extent, which creates a positive feedback loop. A similar argument holds for the sea-ice albedo feedback (Curry et al., 1995; Morassutti, 1991). Traditionally, GCMs have treated high-latitude cryospheric processes quite crudely. However, the recent consciousness of the increased importance of the albedo feedback due to climate change has altered this, and improved parameterization of sea-ice albedo seems to receive high priorities.

Validation and intercomparison projects like Project for Intercomparison of Land-Surface Parameterization Schemes (PILPS), Snow Model Intercomparison Project (SnowMIP) and Sea Ice Model Intercomparison Project (SIMIP) have demonstrated that there are significant differences in the formulation of individual processes concerning snow and sea ice in climate models. Currently, a diversity of snow and sea-ice albedo parameterizations are used in GCMs, see *e.g.* Paper I or Curry et al. (2001); Barry (1996) for an overview. Most parameterizations are very simple, depending on surface type and temperature. A few schemes include snow depth and ice thickness, and even fewer include spectral and solar angle dependencies. Because of the complex high-latitude cryospheric processes and difficulties with describing them in an appropriate manner, many GCMs use the sea-ice albedo as tuning parameter. Much more detailed albedo schemes have been implemented in small scale sea-ice models. In 1993, Ebert and Curry published their thermodynamic sea-ice model with an advanced scheme for sea-ice albedo. In later publications (Schramm et al., 1997; Ebert et al., 1995) the scheme was modified and enhanced, but the basic with five surface types (dry snow, melting snow, bare sea ice, melt ponds and open water) each having a separate parameterization for albedo and the corresponding fraction, remained.

2.4.1 Snow and sea-ice albedo schemes in general

Two main groups of snow albedo schemes are predominant for GCMs; the temperature dependent schemes and the prognostic schemes. The temperature dependent schemes have the albedo varying linearly with the surface temperature between a maximum value at the melting point and a minimum value at cold temperatures. The prognostic albedo scheme has an albedo dependent on the albedo at the previous time step, with separate decay factors for melting and non-melting snow (Figure 2.11b), and reset the albedo to its maximum value for new snowfall above a prescribed precipitation threshold. Both types of schemes can equally well be used for snow on land as for snow covered sea ice, as long as the underlying surface is taken into account. In PILPS Phase 2d the study was focused on modeling of snow, and out of 21 participating models, eight used a prognostic snow albedo scheme, five used an albedo which changed with snow depth, four used a fixed albedo, and the rest used a snow albedo dependence of snow density, temperature or several of the above (Slater et al., 2001). Validation of snow albedo schemes have been performed by Boone and Etchevers (2001); Essery et al. (1999); Slater et al. (1998); Yang et al. (1997). The sea-ice albedo schemes in many GCMs are similar because they treat sea-ice albedo as a linear function of temperature, and also some include the ice thickness as a parameter (Curry et al., 2001). But, unfortunately, every model has its own values for maximum- and minimum albedo as well as the range for linear temperature dependence. Sea-ice albedo schemes have been intercompared and validated in Liu et al. (2007); Køltzow (2007); Curry et al. (2001). Two common deficiencies with the temperature dependent schemes in GCMs are that the albedo is assumed to vary linearly with temperature and that the maximum albedo usually is set too lowMorassutti (1989). It is suggested the best candidates for accurate sea-ice albedo simulations are GCMs with basis in snow and ice characteristics and thickness. Firstly, standardization is required, either based

on a detailed theoretical model of snow and ice albedo or based on integrated satellite-air-ground observations of albedo. Secondly, snow albedo should be made a function of snow grain size, impurities, optical snow depth and underlying surface, while sea-ice albedo should be made a function of ice thickness, brine density, air bubbles, melt pond area and the extent and occurrence of surface drainage. Also, the albedo should be based on cloud cover fraction, cloud optical depth and solar-zenith angle (Morassutti, 1989).

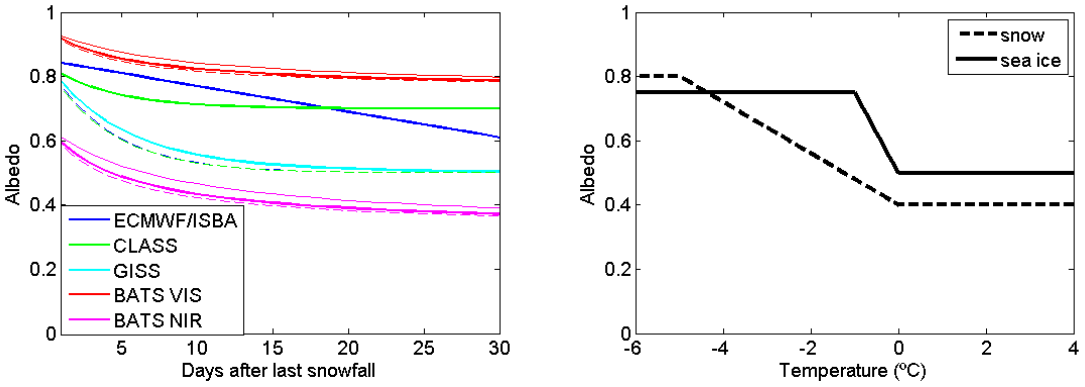

(a) (b)

Figure 2.11: Snow albedo parameterizations in GCMs. (a) The prognostic snow albedo schemes for some GCMs, giving the albedo decay as a function of days since last snow fall. The GCMs are ECHM5 (Roeckner et al., 2003), UKMO (Essery and Yang, 2001; Essery et al., 1999), CLASS (Verseghy, 1991), ISBA (Douville et al., 1995), GISS (Hansen et al., 1983), BATS (Bonan et al., 2002) and ECMWF (ECMWF, 2003) (for a complete descriptions of the schemes we refer to Paper I). The solid lines are for dry snow while the dashed lines are for melting snow. BATS is the only model with two spectral bands (VIS and NIR). The albedo decay for BATS is temperature dependent, and the bold lines are the decay for 0°C, the solid lines for -5°C, and the dashed lines for 5°C. (b) ECHAM5 temperature dependent schemes for snow and sea-ice albedo.

2.4.2 Snow and sea-ice albedo schemes in ECHAM5 GCM

Special focus in this thesis have been on the coupled model consisting of the atmospheric model ECHAM5 (Roeckner et al., 2003, 2006) connected to the ocean model MPI-OM (Marsland et al., 2003). In the coupled model (Jungclaus et al., 2006), the ocean passes to the atmosphere the sea surface temperature, sea-ice concentration, sea-ice thickness, snow depth on ice, and the ocean surface velocities. The atmosphere runs with these boundary values for one coupling time step (one day) and accumulates the forcing fluxes. These fluxes are then transferred to the ocean. All fluxes are calculated separately for ice-covered and open water partitions of the grid cells.

ECHAM5 has a temperature dependent snow and sea-ice albedo scheme, where the albedo is assumed to be a linear function of surface temperature, ranging between a maximum value at the melting point ($T_s = 0°C$) and a minimum value for cold temperatures (below -5°C for snow on land, and below $-1°C$ for sea ice, Figure 2.11a). The maximum and minimum

albedo values for snow on land are 0.80 and 0.30, and for sea ice 0.75 and 0.50, respectively. The snow cover fraction is a function of snow depth $f_s = 0.95 \tanh(100 d_s)$, where d_s is the snow depth in m SWE (Roeckner et al., 2003). The grid mean surface albedo in ECHAM5 depends on the specified background albedo, temperature dependent snow and sea-ice albedos, snow depth, and for land schemes: forest fraction and snow in the canopy. Paper I compares ECHAM5 snow albedo against several other GCMs, as well as validating it against ground truth datasets, while a new and more physically based parameterization scheme for ECHAM5 is the topic of Paper II.

2.5 Validation of climate models

GCMs simulate the day-to-day variations in the weather on short time scales, and climate-variations on longer time scales, and to evaluate the accuracy of any GCM, it can be compared and validated against ground truth observations. For past climates, proxy data (*e.g.*, information on sediment- and/or ice cores) can be converted into physical parameters and used for evaluation of model outputs; for present climate, both ground-based and remotely sensed information can be used. The GCMs are often used for sensitivity studies, *e.g.* by changing a physical parameterization or the boundary conditions. In such context, the experimental run is typically compared against the control run. Even if modifications in the experimental run have no effect on the climate, the difference field between the control and experimental run will deviate from zero and reflect random variations (von Storch and Zwiers, 1999). Similarly, the difference field between simulated and observed climate parameters can exhibit possibly large differences, even if the model is "perfect". Because of this, we propose to apply statistical techniques to distinguish between the deterministic model error and the internal model noise in the validation of climate models.

In order to validate GCMs, we would in principle need to compare the statistics of various variables at temporal and spatial scales against observations. However, it is difficult, if not impossible, to characterize the observed climate in such a way, as the observations are scattered both in time and space. In reality, model validation must be restricted to validation of a few variables of interest. The comparison between simulations and observations, or simulations from control run against a modified run, can be performed with statistical hypothesis tests of the null hypothesis by assuming the two datasets to have the same distribution. However, such testing will suffer from some of the common shortcoming in normal hypothesis testing (Anderson et al., 2000; Germano, 1999; Katz, 1992). In von Storch and Zwiers (1999) it is stated as strongly as "a fully satisfactory verification or validation is impossible within the hypothesis testing paradigm".

Statistical techniques can identify areas in an image where the difference field between a model and the validation data are higher than the noise level, that is, the difference is statistically significant (Chervin and Schneider, 1976). However, for a climatologist, "the practical significance" may be of equal or greater importance. To clarify: statistical significance can be interpreted by asking if the means of two datasets are the same or different, which is typical in hypothesis testing. However, when assessing the practical significance, one needs to quantify the magnitude of the difference. This is because a very small, subtle difference can be found to be statistically significant given a large enough sample size, even though the difference is of little practical importance. The problem with statistical significance is that it may not be particularly meaningful for a given application because of the natural variability

of the phenomena or the arbitrariness of the defined statistical threshold. Experienced climatologists, on the other hand, can decipher whether the difference between, *e.g.*, two albedo datasets are climatologically meaningful, but this process is subjective and greatly depends on the skill of the observer. Also, there is no exact definition of practical significance. Often a normalized albedo difference is used as a measure of practical significance, and values above a pre-described threshold are considered to be practically significant. This topic is exploited further in Paper IV.

2.6 Satellite remote sensing of albedo

The use of optical sensors for remote sensing of the Arctic snow and sea-ice environment are somewhat limited due to the frequent cloud cover. But clear sky events offer the opportunity to measure surface albedo, and attempts have been made with both Moderate Resolution Imaging Spectroradiometers (MODIS), Advanced Very High Resolution Radiometer (AVHRR) and Thematic Mapper (TM) sensors on board Aqua and Terra, NOAA and Landsat satellites, respectively. Albedo, or reflectance, can be measured from space by performing a number of operations on the raw data values of the satellite image. One of the first attempts on deriving surface albedo from satellites used the TM onboard Landsat (Hall et al., 1989). Algorithms for sea-ice albedo have also been constructed from AVHRR in the early-mid 1990 by both Lindsay and Rothrock (1994); De Abreu et al. (1994).

A common method that has been widely used for *e.g.* TM and AVHRR is reviewed by König et al. (2001) and includes first to convert the raw data to spectral radiance (reflected energy). The planetary reflectance is calculated as the reflected energy divided by the incoming solar energy, and needs to be corrected for atmospheric conditions (Tanré et al., 1990). The satellites measure reflectance in the look direction of the sensor. Snow reflects anisotropically due to its BRDF characteristics (section 2.1.1), and this must be corrected for in order to calculate the reflectance integrated over all angles. The total albedo is the narrowband reflectance integrated over the full solar spectrum (Equation (2.2)). Two approaches for narrowband to total conversion is commonly used: (i) to interpolate the satellite reflectance in the visible part of the spectrum and model the reflectance in the NIR to get the satellite reflectance for the full solar spectrum, or (ii) to use an empirical relation between the narrowband reflectance and total albedo (Knap et al., 1999). The drawback with the second approach is that it is normally only applicable for the site and surface type it was developed for.

2.6.1 MODIS

The MODIS sensor is well suited for monitoring albedo from space as it images mid-to-high latitude snow and sea-ice covered areas with high spatial- and fine spectral resolution on a daily basis. The MODIS sensor has 7 bands in the visible and near infra-red and a pixel resolution of 250-500 meters (MODIS, 2005). A MODIS snow albedo product (MOD10) was developed by Klein and Stroeve (2002) using existing MODIS products for determining the directional surface reflectance for cloud free and snow covered pixels. For glacier, tundra and prairie pixels, a snow BRDF was used to account for anisotropies, while the anisotropy of forest was ignored. Narrow-to-broadband conversion schemes were conducted to calculate the total albedo. The snow albedo product is based on the MOD09 directional surface reflectance product, which, unfortunately, is not optimized for bright surfaces (Vermote and Vermeulen,

1999), however, MOD10 albedo was evaluated over the Greenland Ice Sheet and found to follow the general seasonal variability well, however it exhibited more temporal variability than observed (Stroeve et al., 2006).

Liang et al. (2005) developed an improved version of a direct estimation algorithm (DEA) for snow albedo from MODIS. The DEA link the top-of-the-atmosphere MODIS observations directly to the surface albedo through regression techniques, and thereby reduce errors associated with the individual steps in *e.g.* MOD10. The algorithm is only recommended for solar zenith angles less than 70° (Stroeve et al., 2006; Liang et al., 2005). Comparisons with a limited set of Greenland albedos showed to be very promising, with mean biases of less than 0.02 (Liang et al., 2005). Also, the DEA snow albedo appeared to match Greenland *in situ* albedos better than the MOD10 albedo, however a systematic underestimation was found in spring (Stroeve et al., 2006).

A 16-days MODIS BRDF/albedo product (MOD43) was developed by Schaaf et al. (2002), and used a kernel driven linear BRDF model to describe the anisotropy of the surface reflectance. For locations were a full BRDF model could not be retrieved, a backup-algorithm was used. The main albedo algorithm gives an accuracy of snow albedo within 5%, while the backup-algorithm have lower accuracy (8-11%). In contrast to MOD10, MOD43 provides the white sky and black sky albedo (Equation (2.4)). A 16-days averages of MOD10 were compared against MOD43 albedo, and the mean biases (correlation) were 0.04 (0.89) for black sky albedo and 0.08 (0.87) for white sky albedo (Stroeve et al., 2006) for data from the Terra satellite. The main drawback with the 16-days average product is, however, the rapid albedo changes during spring melting and fall freeze up, which limits its use to long term climate studies.

No operational product for MODIS sea-ice albedo exists, however, we propose one in Appendix B.

3 Motivations and Main Conclusions for Papers I-IV

Paper I:
Intercomparison and Validation of Snow Albedo Parameterization Schemes in Climate Models

C. A. Pedersen and J.-G. Winther, *Climate Dynamics*, 2005, 25: 351-362

Motivation

The main motivation for paper I is twofold: first to intercompare different snow albedo parameterization schemes, and second to validate how accurate they are in their description of snow albedo. No emphasis is put on the ECHAM5 albedo scheme compared to the other six investigated schemes. The significant parameters for describing snow albedo are identified by means of a multiple linear regression model.

Results and main conclusions

Six GCM snow albedo parameterization schemes are intercompared and validated against 59 years of data from eight sites. The model albedos had larger variations than the observations, indicating that existing schemes are too sensitive to certain snow physical and textural properties. This is evident particularly during the winter snow metamorphosis when the model snow albedos for most models decrease by a faster rate or a larger magnitude than the observed snow albedo. For most investigated sites the modeled snow albedos are underestimated during winter and late autumn. However, as the data are from point validation sites from relative flat and open landscapes, the observations probably represent an upper threshold for snow albedo. For the spring snow melting and autumn snow accumulation, the models overestimate the albedo.

The two main types of snow albedo schemes (temperature and prognostic) are compared. The temperature dependent schemes incorrectly fix the snow albedo at certain threshold values depending on the surface temperature. Especially for temperate sites, where the temperature reaches the upper threshold at 0°C several times during the winter without the albedo dropping much, this effect become dominant and unrealistic. The prognostic schemes for snow albedo prove to describe the albedo decay due to snow aging and melting in a more realistic way than the temperature dependent schemes; however, the drawback is that all GCMs support slightly different schemes with different adjusting parameters. The significant parameters for

modeling snow albedo from a multiple regression model are identified as temperature, positive degree day, snow depth, cloud cover and a dummy of snow fall.

Paper II:
A New Sea-Ice Albedo Parameterization for ECHAM5 General Circulation Model

C. A. Pedersen, E. Roeckner, M. Lüthje, J.-G. Winther, in preparation for Journal of Geophysical Research

Motivation

The average temperatures in the Arctic has increased with a factor two of the global average the last 100 years due to global warming. With the increased warming, the effect of the sea-ice albedo feedback is enhanced (Curry et al., 1995; Morassutti, 1991). However, substantial shortcoming exists with respect to today's parameterization of sea-ice albedo in GCMs, as they are inadequate to describe the recent decrease in sea ice in the Arctic (Curry et al., 2001; Morassutti, 1989). We have developed a new sea-ice albedo parameterization scheme for the general circulation model ECHAM5 with takes into account important physical processes for the sea-ice albedo development, *e.g.* by including melt ponds as a separate phase.

Results and main conclusions

The new sea-ice albedo scheme for ECHAM5 separates between snow covered sea ice, bare sea ice, melt ponds and open water, and provides parameterizations for the albedos and fractions, also including the spectral dependency and the effect of clouds. The new scheme is found to reduce the sea-ice albedo both in winter due to snow ageing and in summer due to melt ponds. It simulates the annual cycle of sea-ice albedo in a realistic way by capturing the changes to determine the onset of melt, the duration of melt and the start of the fall freeze-up. The correlation coefficient between one year sea-ice albedo simulations in Arctic multi year ice and one year observations at the SHEBA site (Perovich et al., 2002a) was 0.83, with simulated albedos slightly higher than observed albedo in summer. ECHAM5 modeled the melt pond coverage in accordance with observation at the SHEBA site both when concerning the temporal evolution and the mean area coverage. For the entire northern hemisphere the coverage is on the lower side compared to observations, but it provided, for the first time to our knowledge, an estimate of the spatial variability of the melt pond coverage. The effect on the sea-ice albedo from the new scheme averaged over 50 years in the northern hemisphere was largest in summer, with average reductions of 23%, or 0.14, in August. In the southern hemisphere the reductions were less. The reduced sea-ice albedo leads to overall reduced sea-ice thickness, concentration and volume, with large temporal and spatial variations. *E.g.* some areas experience increased sea-ice albedo in March, resulting in an increasing sea-ice thickness and concentration. In September the pattern is spatially homogeneously with reduced sea-ice albedo, thickness and concentrations. In spite of the new albedo scheme having a large impact on the Arctic sea-ice environment, the global climate parameters remain relatively unchanged.

Paper III:
Combined Airborne Profiling over Fram Strait Sea Ice: Fractional Sea-Ice Types, Albedo and Thickness Measurements

C. A. Pedersen, R. Hall, S. Gerland, A. H. Sivertsen, T. Svenøe and C. Haas, submitted to *Cold Regions Science and Technology*, Oct. 2007

Motivation

The heterogeneous sea-ice cover in the Arctic plays an important role for the climate system, and it is important to have appropriate techniques to get sufficient data (both in quality and quantity) to monitor the sea-ice environment. Such a task would be impossible to carry out with *in-situ* field measurements due to the inaccessibility of these remote areas, and also because it would be too time consuming. Optical remote sensors offer the possibility to estimate some sea-ice parameters, however, their use is limited due to frequent cloud covers in the Arctic (particularly in spring). Instead, we propose to monitor the sea-ice environment from airborne measurements. We present a framework to measure fractional sea-ice types, albedo and sea-ice thickness. Such a comprehensive dataset would in addition be very useful in the context of validating GCM climate parameters or other remote sensing datasets.

Results and main conclusions

The paper describes the data collected and the techniques used to analyze the airborne sea-ice data from an expedition from the marginal ice zone into the multiyear ice in the Fram Strait in spring 2005 to measure sea-ice types, albedo and thickness. A combination of methods is used to extract more information from each data set compared to what originally and traditionally are obtained. The principal information from the applied methods gave the sea-ice types from digital photography, the spectral and broadband reflectance factor from the spectrometer measurements and the ice thickness profile from the electromagnetic-"bird" measurements, with emphasize on using, adapting and combining techniques. The digital images are standardized, textural features are extracted and a trained neural network is used for classification. The optical measurements are normalized and standardized to minimize effects from the set up and atmospheric conditions.

The fractional sea-ice types prove to have large spatial variability, with average fractions for snow covered sea-ice of 81.0%, thick bare ice 4.0%, thin ice 5.3% and open water 9.6%, hence an average ice concentration of 90.3%. The average broadband reflectance factor is 0.73 with standard deviation of 0.33, while the mean total sea-ice thickness (including snow) is 2.1 m with a standard deviation 1.3 m. We also found a relative high correlation (0.69) between the measured albedo and sea-ice concentration.

The study shed light on the enormous potential of integrated airborne surveys over sea ice with modern methods. With improvements on the individual set-ups and steps, we can reduce the temporal and spatial bias, particularly concerning the optical measurements.

Paper IV:
A Scale-Space Approach for Detecting Significant Differences between Models and Observations Using Global Albedo Distributions

C. A. Pedersen, F. Godtliebsen, A. C. Roesch, *Journal of Geophysical Research*, Accepted, Dec. 2007

Motivation

The validation of climate models has traditionally required an experienced climatologist investigating the difference field between the climate model output and some appropriate validation dataset. However this process is both subjective and greatly depending on the skill of the observer. When climate models are used for sensitivity studies, *e.g.* by changing a physical parameterization, the validation will involve comparing the experimental run against a control run. In such experiments the difference field between the control and experimental run will often be nonzero and reflect random variations, even if the modifications have no direct effects on the climate. Similarly, the difference field between simulated and observed climate parameters can exhibit, possible, large differences even if the model is "perfect". We therefore feel it is highly necessary to apply statistical techniques to distinguish between the deterministic model error and the internal model noise in the validation process. This paper propose an objective and fully automatic statistical technique for such problems by adapting existing scale-space methodology.

Results and main conclusions

We have developed a consistent and fully automatic adapted significance-in-scale-space methodology for detecting significantly differences between a GCM model output parameter and the corresponding validation data. The suggested technique detects areas or pixels in a difference image between model and validation data, significantly different from zero taking into account the inter-annual variability and by correcting for multiple testing. The technique determines significantly differences at a wide range of scales or spatial resolution, thereby avoiding the problem of choosing an optimal scale.

The methodology is successful in detecting significant differences between ECHAM5 surface albedo and the remote-sensing PINKER surface albedo climatology. Overall, the ECHAM5 model overestimates the albedo compared to the PINKER climatology for all scales in March, with snow and ice covered areas having the largest discrepancies. At the finest scales (280 km) very few areas of significantly albedo differences are detected because of relatively high interannual variability for the areas of largest difference, such as major parts of snow-covered Northern Eurasia, North America and the Southern Ocean. At 1100 km, significant albedo differences are found in the southern part of the Arctic Ocean adjacent to the ice edge as caused by the different positions of the ice edge in ECHAM5 and PINKER. The scale 2500 km proves to be reasonable for validating the albedo scheme, as most of the snow-covered regions in Northern Eurasia with positive differences above 0.2, and relative low interannual variability are marked as significant.

Overall, the adapted significance in scale-space technique proves to be a powerful and easy approach for detecting significantly different areas, and it will be a helpful tool for doing

objective inference for a climatologist facing large amount of climate data to validate and intercompare (cf. IPCC, AR4).

4 Future Work

The thesis has a wide focus in the sense that it concerns many aspects of optical properties of snow and ice, including *in situ* and airborne measurements, to some extent remote sensing of optical properties, as well as parameterization of snow and sea-ice albedo and validation of climate models in general. However, there are some areas where more investigations will be useful:

- The new sea-ice albedo scheme for ECHAM5 have so far only been implemented in the coarse-scale T31 model. We also plan to do simulations with the fine-scale T63 resolution model. However, because the models operate on different scales, they are not identical in their performance. The main difference is that the meridional heat transport in both the atmosphere and ocean is underestimated at coarse resolution. For example, the meridional overturning in the North Atlantic is almost 30% smaller in the T31 than in the T63 model (E. Roeckner, personal communication). The new albedo scheme somehow compensates for the underestimated heat transport in T31. Therefore the crucial test will be to see how the T63 model reacts. We also want to run the model with present day climate forcing in order to see how well the new sea-ice albedo scheme describe present day albedo evolution.

- The possibilities lying in remote sensing of the Earth surface have not been used to its full potential in this thesis. We have developed a global, daily sea-ice albedo product based on the Moderate Resolution Imaging Spectroradiometer (MODIS) (Appendix B); however, we have not been able to validate it due to lack of suitable validation data. Airborne measurements such as investigated in Paper III, are appropriate for such a task. But, a main problem is that optical sensors like MODIS requires clear sky, and hence the validation data needs to be collected under such conditions. For the campaign to the Fram Strait in spring 2005, which Paper III is based on, the sky was overcast for the whole period; hence these data can not be used for validating the MODIS sea-ice albedo. This is a task we want to pursuit further.

- An important question regarding remote sensing, which was not raised in this thesis, is how remote sensing albedo products can be utilized as input to climate models. This deserves further study.

- Black Carbon (BC) particles emitted by fossil fuel and incomplete biomass combustion are transported to the Arctic where they deposit in snow and ice and lead to reduced surface albedo, thus contributes to warming of the climate. However, it is not straight foreword to derive the alteration on albedo from BC in snow because of the relative low natural concentrations of BC, and the natural variabilities of albedo due to the snow physical and environmental factors. We will pursuit this further in future research.

- In connection with the BC survey above, we plan to use state-of-the-art technology to measure albedo over a wide range of Arctic terrain with an Un-manned Aerial Vehicle (UAV). The UAV platform offer the possibility to collect huge amounts of data, without the limitations of remote sensing from satellites (*e.g.* clouds). The primary goals are to establish highest quality measurements of Arctic albedo and background variability, and to quantify induced changes of albedo over snow and ice surfaces driven by transport and deposition of pollutants.

5 Concluding Remarks

Today we experience an accelerated melting of sea ice in the Arctic which the General Circulation Models (GCMs) are inadequate to predict (Wang et al., 2006; Parkinson et al., 2006; Køltzow, 2007). We believe one of the reasons is the shortcomings in the sea-ice albedo schemes for these GCMs. Sea-ice albedo parameterizations have huge potential for improvements, and consequently the main motivation behind this thesis has been to develop and implement a new physically based scheme for sea-ice albedo in ECHAM5 GCM. The new sea-ice albedo parameterization includes important components like albedo decay due to snow ageing, bare sea-ice albedo dependent on ice thickness and an explicit treatment of melt pond albedo dependent on melt pond depth and fractional coverage. The thesis has also dealt with validation of GCMs in general, both concerning measurements for which to validate against, and techniques for performing the validation.

In the introduction we placed four main scientific questions which were the governing idea throughout this thesis. Here we combine and summarize the results and knowledge from the four papers and three appendices.

1. Which parameters affect the optical properties of snow and sea ice, in what ways, and which are important parameters for modeling the snow and sea-ice albedo?

Snow and ice physical parameters affect the optical properties of snow and sea ice in various ways. Snow grain size is one of the most important parameters describing the decay in snow albedo during snow metamorphosis. The snow depth is crucial for snow albedo for thin snow covers, and must be included in a fractional representation. The spectral properties depend on wavelength (overall the albedo is reduced for increasing wavelength, with a few absorption bands due to ice absorption), cloud cover (the albedo increases with more clouds) and solar angle (the albedo increases with increasing solar zenith angle). Based on field measurements and regression modeling the statistical significant parameters for modeling snow albedo are temperature, positive degree day, snow depth, cloud cover and dummy of snow fall (Paper I). For the sea-ice counterpart, temperature, snow depth, cloud cover and a dummy for snow depth are significant (Appendix A). The latter result is due to the snow that completely covers the sea ice in winter, hence the snow parameters dominate. The new physically based sea-ice albedo scheme for ECHAM5 separates between snow covered sea ice, bare sea ice, melt ponds and open water (with distinct parameterizations for albedos and the corresponding fractions). Separate schemes are developed for two wavelength bands and diffuse and direct radiation. Based on results from Paper I, the snow component in the new albedo parameterization use the sophisticated BATS snow albedo scheme which includes the temperature effect in a prognostic equation for the snow age, and accounts for grain growth, solar angle and aerosols (Dickinson et al., 1993). The bare sea-ice albedo increases exponentially with the ice thickness (Brandt et al., 2005), while the melt pond albedo is determined from the melt pond depth (Morassutti

and Le Drew, 1996). The melt pond depth is not a standard parameter in ECHAM5, so it is modeled from the daily surface ice melt rate. The melt pond fraction is calculated from the melt pond depth by using relations from a small-scale melt pond model (Lüthje et al., 2006).

2. How does the new and more physically based sea-ice albedo scheme in ECHAM5 modify the climate simulations, particularly for the sea-ice environment?

The new sea-ice albedo scheme in ECHAM5 GCM (Paper II) overall reduces the sea-ice albedo both in winter due to snow ageing and in summer due to melt ponds. The explicit treatment of melt pond albedos represents a substantial improvement when simulating the annual cycle of sea-ice albedo by capturing the onset of melt, the duration of melt and the start of the fall freeze-up. The reductions in sea-ice albedo are statistically significant, principally in northern hemisphere during summer. The effect of reduced sea-ice albedo is overall reduced sea-ice thickness, concentration and volume, with relative large temporal and spatial variations. In March, some areas experience increased albedo, resulting in thicker sea ice and higher ice concentration, however, in September, the overall pattern is spatially homogeneous with reduced albedo, thickness and concentrations everywhere. For some areas the reductions in the northern hemisphere are statistically significant, mostly for sea-ice thickness, but also for sea-ice areas in summer. Areas of significantly differences are not found for sea-ice thickness nor area in the southern hemisphere, confirming that melt ponds play a minor role in Antarctica. Despite the relative large effects from the new albedo scheme on the sea-ice environment, the changes on the global climate are minor.

3. How can optical measurements (both *in situ*, airborne and remote sensing) of snow and sea ice be used and combined to describe the Arctic sea-ice environment and provide valuable information for validation purposes?

The collection and processing of large amounts of optical data are one of the main issues throughout this thesis. Both small scales (in-situ measurements), regional scales (airborne measurements) and global scales (remote sensing measurements) are investigated, providing information of optical properties of snow and sea ice at different resolutions and foot-prints. The small scale measurements are utilized for point-site validation, process studies and development of characteristic properties (characteristic albedo curves). Both the airborne and remote sensing measurements require substantial data processing before the albedo can be extracted; however, both products are suitable for validation of GCMs or (other) remote sensing products. The processing and combinations of airborne digital photograph, optical measurements and electromagnetic measurements are the focus of Paper III. Together such measurements describe the sea-ice environment and provide fractional sea-ice types, sea-ice albedo and sea-ice thickness, thus also sea-ice extent and volume. Daily global area fractions and sea-ice albedo products based on MODIS remote sensor are also developed (Appendix B). The albedo processing required correction for atmospheric scattering, absorption and anisotropic effects, classification of surface types and narrow- to broad band conversion, while the area fractions are calculated from characteristic albedo spectra and spectral unmixing procedures (Vikhamar, 2003). However, the frequent cloud cover in Arctic, particularly in spring, limits the use of the MODIS to only clear sky days.

4. Which techniques can be used for validating climate models in an appropriate and consistent way?

The validation of climate models is not straight forward and requires statistical methodology. Previously, the validation of climate models has required an experienced climatologist investigating the difference field between climate model simulations and an appropriate validation dataset. In Paper IV we develop a consistent and fully-automatic adapted significance-in-scale-space methodology for detecting statistically significant differences between GCM model output and validation data. For such validation the scaling issue is important, as for smaller scales there is usually a large amount of noise, and for coarser scales the interesting features are smoothed away. The suggested technique avoids the ambiguity as it determines significantly differences over a wide range of scales.

References

D. R. Anderson, K. P. Burnham, and W. L. Thompson. Null Hypothesis Testing: Problems, Prevalence, and an Alternative. *Journal of Wildlife Management*, 64(4):912–923, 2000.

D. G. Baker, R. H. Skaggs, and D. L. Ruschy. Snow Depth Required to Mask the Underlying Surface. *Journal of Applied Meteorology - Notes and Correspondence*, 30:387–392, 1991.

R. G. Barry. The Parameterization of Surface Albedo for Sea Ice and its Snow Cover. *Progress in Physical Geography*, 20(1):63–79, 1996.

C. E. Bøggild, M. Lüthje, and J. Holmes. Albedo Observations with Large Concentrations of Black Carbon in High Arctic Snow Packs from Svalbard. In *63rd Eastern Snow Conference, Newark, Delaware, USA*, 2006.

C. F. Bohren and B. R. Barkstrom. Theory of the Optical Properties of Snow. *Journal of Geophysical Research*, 79(30):4527–4534, October 1974.

C. F. Bohren and D. R. Huffman. *Absorption and Scattering of Light by Small Particles*. John Wiley & Sons, Inc., 1983.

G. B Bonan, K. W. Oleson, M. Vertenstein, S. Levis, X. Zeng, Y. Dai, R. E. Dickinson, and Z.-L. Yang. The Land Surface Climatology of the Community Land Model Coupled to the NCAR Community Climate Model. *Journal of Climate*, 15:3123–3149, 2002.

A. Boone and P. Etchevers. An Intercomparison of Three Snow Schemes of Varying Complexity Coupled to the Same Land Surface Model: Local-Scale Evaluation at an Alpine Site. *Journal of Hydrometeorology*, 2:374–394, 2001.

R. E. Brandt, S. G. Warren, A. P. Worby, and T. C. Grenfell. Surface Albedo of the Antarctic Sea Ice Zone. *Journal of Climate*, 18:3606–3622, 2005.

R. M. Chervin and S. H. Schneider. On Determining the Statistical Significance of Climate Experiments with general Circulation Models. *Journal of the Atmospheric Science*, 33(3): 405–412, 1976.

J. Curry, J. L. Schramm, and E. E. Ebert. Sea Ice-Albedo Climate Feedback Mechanism. *Journal of Climate*, 8:240–247, February 1995.

J. A. Curry, J. L. Schramm, D. K. Perovich, and J. O. Pinto. Applications of SHEBA/FIRE Data to Evaluation of Snow/Ice Albedo Parameterizations. *Journal of Geophysical Research*, 106(D14):15345–15355, July 2001.

R. A. De Abreu, J. Key, J. A. Maslanik, M. C. Serreze, and E. F. Le Drew. Comparison of *In Situ* and AVHRR-Derived Broadband Albedo over Arctic Sea-Ice. *Arctic*, 47(3):288–297, 1994.

R. E. Dickinson, A. Henderson-Sellers, and P. J. Kennedy. Biosphere Atmosphere Transfer Scheme (BATS) Version 1e as Coupled to the NCAR Community Climate Model. Technical report, NCAR Technical Note NCAR/TN-387+STR, 1993. 72 pp.

H. Douville, J.-F. Royer, and J.-F. Mahfouf. A New Snow Parameterization for the Météo France Climate Model. *Climate Dynamics*, 12:21–35, 1995.

E. E. Ebert, J. L. Schramm, and J. A. Curry. Disposition of Solar Radiation in Sea Ice and the Upper Ocean. *Journal of Geophysical Research*, 100(C8):15965–15975, August 1995.

ECMWF, 2003. European Centre for Medium-Range Weather Forecasts. http://www.ecmwf.int/research/ ifsdocs/PHYSICS/, 2003. Accessed September, 2003.

I. Eisenman, N. Untersteiner, and J. S Wettlaufer. On the Reliability of Simulated Arctic Sea Ice in Global Climate Models. *Geophysical Research Letter*, 34(L10501), 2007. doi:10.1029/2007GL029914.

R. Essery and Z.-L. Yang. An Overview of Models Participating in the Snow Model Intercomparison Project (SnowMIP). SnowMIP Workshop, 8th Scientific Assembly of IAMAS, Innsbruck, 2001.

R. Essery, E. Martin, H. Douville, A. Fernández, and E. Brun. A Comparison of Four Snow Models Using Observations from an Alpine Site. *Climate Dynamics*, 15:583–593, 1999.

M. G. Flanner, C. S. Zender, J. T. Randerson, and P. J. Rasch. Present-day Climate Forcing and Response from Black Carbon in Snow. *Journal of Geophysical Research*, 112(D11202), June 2007.

S. Gerland, Winther J.-G., and J.-B. Ørbæk. Physical Properties, Spectral Reflectance and Thickness Development of First Year Fast Ice in Kongsfjorden, Svalbard. *Polar Reaserch*, 18(2):275–282, 1999a.

S. Gerland, J.-G. Winther, J. B. Ørbæk, G. E. Liston, N. A. Øritsland, A. Blanco, and B. Ivanov. Physical and Optical Properties of Snow Covering Arctic Tundra on Svalbard. *Hydrological Processes*, 13:2331–2343, 1999b.

S. Gerland, G. E. Liston, J.-G. Winther, J. B. Ørbæk, and B. V. Ivanov. Attenuation of Solar Radiation in Arctic Snow: Field Observations and Modelling. *Annals of Glaciology*, 31: 364–368, 2000.

S. Gerland, C. Haas, M. Nicolaus, and J.-G. Winther. Seasonal Development of Structure and Optical Properties of Fast Ice in Kongsfjorden, Svalbard. In C. Wiencke, editor, *The Coastal Ecosystems of Kongsfjorden, Svalbard*, number 492, pages 26–34. Alfred Wegner Institute for Polar & Marine Research, 2004.

S. Gerland, J. Aars, T. Bracegirdle, E. Carmack, H. Hop, G. K. Hovelsrud, K. M. Kovacs, C. Lydersen, D. K. Perovich, J. Richter-Menge, S. Rybråten, H. Strøm, and J. Turner.

Global Outlook for Ice and Snow, chapter Ice in the Sea (Chapter 5), pages 63–96. UN Environment Program (UNEP), 2007.

J. D Germano. Ecology, Statistics, and the Art of Misdiagnosis: The need for a Paradigm Shift. *Environmental Review*, 7:167–190, 1999.

T. Grenfell. A Theoretical Model of the Optical Properties of Sea Ice in the Visible and Near Infrared. *Journal of Geophysical Research*, 88(C14):9723–9735, 1983.

T. Grenfell and D. K. Perovich. Seasonal and Spatial Evolution of Albedo in a Snow-Ice-Land-Ocean Environment. *Journal of Geophysical Research*, 109(C1):1–15, 2004.

T. C. Grenfell and D. K. Perovich. Spectral Albedos of Sea Ice and Incident Solar Irradiance in the Southern Beaufort Sea. *Journal of Geophysical Research*, 89(C3):3573–3580, 1984.

T. C. Grenfell, S. G. Warren, and P. C. Mullen. Reflection of Solar Radiation by the Antarctic Snow Surface at Ultraviolet, Visible and Near-Infrared Wavelengths. *Journal of Geophysical Research*, 99(D9):18669–18684, 1994.

T. G. Grenfell and G. A. Maykut. The Optical Properties of Ice and Snow in the Arctic Basin. *Journal of Glaciology*, 18(80):225–463, 1977.

D. K. Hall, A. T. C. Chang, J. L. Foster, C. S. Benson, and W. M. Kovalick. Comparison of *In Situ* and Landsat Derived Reflectance of Alaskan Glaciers. *Remote Sensing of Environment*, 28:23–31, 1989.

J. M. Hanesiak, D. G. Barber, R. A. De Abreu, and J. J. Yackel. Local and Regional Albedo Observations of Arctic First-Year Sea Ice during Melt Ponding. *Journal of Geophysical Research*, 106(C1):1005–1016, 2001.

J. Hansen, G. Russell, D. Rind, P. Stone, A. Lacis, S. Lebedeff, R. Ruedy, and L. Travis. Efficient Three-Dimensional Global Models for Climate Studies: Model I and II. *Monthly Weather Review*, 111(4):609–662, 1983.

M. Z. Jacobsen. Climate Response of Fossil Fuel and Biofuel Soot, Accounting for Soot's Feedback to Snow and Sea Ice Albedo and Emissivity. *Journal of Geophysical Research*, 109(D21201), November 2004.

J. H. Jungclaus, N. Keenlyside, M. Botzet, H. Haak, J.-J. Luo, M. Latif, J. Marotzke, U. Mikolajewicz, and E. Roeckner. Ocean Circulation and Tropical Variability in the Coupled Model ECHAM5/MPI-OM. *Journal of Climate*, 19:3952–3972, 2006.

R. W. Katz. Role of Statistics in the Validation of General Circulation Models. *Climate Research*, 2:35–45, July 1992.

A. G. Klein and J. Stroeve. Development and Validation of a Snow Albedo Algorithm for the MODIS Instrument. *Annals of Glaciology*, 34:45–52, 2002.

W. H. Knap, C. H. Reijmer, and J. Oerlemans. Narrowband to Broadband Conversion of Landsat TM Glacier Albedos. *International Journal of Remote Sensing*, 20(10):2091–2110, 1999.

M. Køltzow. The Effect of a New Snow and Sea Ice Albedo Scheme on Regional Climate Model Simulations. *Journal of Geophysical Research*, 112(D07110), April 2007.

M. König, J.-G. Winther, and E. Isaksson. Measuring Snow and Glacier Ice Properties from Satellite. *Reviews of Geophysics*, 39(1):1–27, 2001.

Labsphere, 2007. http://www.labsphere.com/, 2007. Accessed November 2007.

S. Liang, J. Stroeve, and J. E. Box. Mapping Daily Snow/Ice Shortwave Broadband Albedo from Moderate Resolution Imaging Spectroradiometer (MODIS): The Improved Direct Retrieval Algorithm and Validation with Greenland In Situ Measurements. *Journal of Geophysical Research*, 110(D10109), 2005.

R. W. Lindsay and D. A Rothrock. Arctic Sea Ice Albedo from AVHRR. *Journal of Climate*, 17:1737–1749, 1994.

J. Liu, Z. Zhang, J. Inoue, and R. M. Horton. Evalution of Snow/Ice Albedo Parameterizations and Their Impacts on Sea Ice Simulations. *International Journal of Climatology*, 27:81–91, June 2007.

M. Lüthje, D. L. Feltham, P. D. Taylor, and M. G. Worster. Modeling the Summertime Evolution of Sea-Ice Melt Ponds. *Journal of Geophysical Research*, 111(C02001), 2006.

S. J. Marsland, H. Haak, J. H. Jungclaus, M. Latif, and F. Röske. The Max-Planck-Institute Global Ocean/Sea Ice Model with Orthogonal Curvilinear Coordinates. *Ocean Modelling*, 5:91–127, 2003.

R. A. Massom, H. Eicken, C. Haas, M. O. Jeffries, M. R. Drinkwater, M. Sturm, A. P. Worby, X. Wu, V. I. Lytle, S. Ushio, K. Morris, P. A. Reid, S. G. Warren, and I. Allison. Snow on Antarctic Sea Ice. *Reviews of Geophysics*, 39(3):413–445, August 2001.

MODIS, 2005. Moderate Resolution Imaging Spectroradiometer (MODIS). http://modis.gsfc.nasa.gov/, 2005. Accessed May, 2005.

M. P. Morassutti. Surface Albedo Parameterization in Sea Ice Models. *Progress in Geophysical Geography*, 13:348–366, 1989.

M. P. Morassutti. Climate Model Sensitivity to Sea Ice Albedo Parameterization. *Theoretical Applied Climatology*, 44:25–36, 1991.

M. P. Morassutti and E. F. Le Drew. Albedo and Depth of Melt Ponds on Sea Ice. *International Journal of Climatology*, 16:817–838, 1996.

F. E. Nicodemus, J. C. Richmond, I. W. Ginsberg, and T. Limperis. Geometrical Considerations and Nomenclature for Reflectance. Technical report, U.S. Department of Commerce, National Bureau of Standards, 1977.

H. C. Ohanian. *Physics*, volume 1. W. W. Northon and Company inc, NY, second edition, 1989. ISBN: 0-393-95750-0.

C. L. Parkinson, K. Y. Vinnikov, and D. J. Cavalieri. Evaluation of the Simulation of the Annual Cycle of Arctic and Antarctic Sea Ice Coverages by 11 Major Global Climate Models. *Journal of Geophysical Research*, 111(C07012), 2006.

D. K. Perovich. *UV Radiation and Arctic Ecosystems*, chapter Ultraviolet Radiation and the Optical Properties of Sea Ice and Snow. Springer-Verlag Berlin Heidelberg, 2002. Ecological Studies, Vol 153.

D. K. Perovich. Light Reflection from Sea Ice During the Onset of Melt. *Journal of Geophysical Research*, 99(C2):3351–3359, 1994a.

D. K. Perovich. The Optical Properties of Sea Ice. Physics of Ice-Covered Seas, Volume I. Lecture notes from a summer school in Savonlinna, Finland, 6-17. June, 1994b.

D. K. Perovich. Observations of the Polarization of Light Reflected from Sea Ice. *Journal of Geophysical Research*, 103(C3):5563–5575, 1998.

D. K. Perovich, C. S. Roesler, and W. S. Pegau. Variability in Arctic Sea Ice Optical Properties. *Journal of Geophysical Research*, 103(C1):1193–1208, 1998.

D. K. Perovich, T. C. Grenfell, B. Light, and P. V. Hobbs. Seasonal Evolution of the Albedo of Multiyear Arctic Sea Ice. *Journal of Geophysical Research*, 107(C10), 2002a.

D. K. Perovich, W. B. III Tucker, and K. A. Ligett. Aerial Observations of the Evolution of Ice Surface Conditions during Summer. *Journal of Geophysical Research*, 107(C10):8048–8062, October 2002b.

J. W. Pomeroy and D. M. Gray. *Snowcover. Accumulation, Relocation and Management.* NHRI Science Report No. 7, 1995.

K. Rasmus, J. Ehn, M. Granskog, E. Kärkäs, M. Leppäranta, A. Lindfors, A. Pelkonen, S. Rasmus, and A. Reinart. Optical Measurements of Sea Ice in the Gulf of Finland. *Nordic Hydrology*, 33(2/3):207–226, 2002.

W. G. Rees. *Remote Sensing of Snow and Ice.* Taylor & Francis, 2006.

E. Roeckner, G. Bäuml, L. Bonaventura, R. Brokopf, M. Esch, M. Giorgetta, S. Hagemann, I. Kirchner, L. Kornblueh, E. Manzini, A. Rhodin, U. Schlese, U. Schulzweida, and A. Tompkins. The Atmospheric General Circulation Model ECHAM5 - Part 1. Technical Report 349, Max Planck Institute for Meteorology, 2003.

E. Roeckner, R. Brokopf, M. Esch, M. Giorgetta, S. Hagemann, L. Kornblueh, E. Manzini, U. Schlese, and U. Schulzweida. Sensitivity of Simulated Climate to Horizontal and Vertical Resolution in the ECHAM5 Atmosphere Model. *Journal of Climate*, 19:3771–3791, 2006.

C. B. Schaaf, F. Gao, A. H. Strahler, W. Lucht, X. Li, T. Tsang, N. C. Strugnell, X. Zhang, Y. Jin, J.-P. Muller, P. Lewis, M. Barnsley, P. Hobson, M. Disney, G. Roberts, M. Dunderdale, C. Doll, R. P. d Éntremont, B. Hu, S. Liang, J. L. Privette, and D. Roy. First Operational BRDF, Albedo Nadir Reflectance Products from MODIS. *Remote Sensing of Environment*, 83:135–148, 2002.

J. L. Schramm, M. M. Holland, J. A. Curry, and E. E. Ebert. Modeling the Thermodynamics of a Sea-Ice Thickness Distribution - 1. Sensitivity to Ice Thickness Resolution. *Journal of Geophysical Research*, 102(C10):23079–23091, October 1997.

Secretary of World Meteorological Organization. WMO Sea-Ice Nomenclature. Technical report, World Meteorological Organization, 1970.

A. G. Slater, A. J. Pitman, and C. E. Desborough. The Validation of a Snow Parameterization Designed for Use in General Circulation Models. *International Journal of Climatology*, 18: 595–617, 1998.

A. G. Slater, C. A. Schlosser, C. E. Desborough, A. J. Pitman, A. Henderson-Sellers, A. Robock, K. Y. Vinnikov, K. Mitchell, A. Boone, H. Braden, F. Chen, P. M. Cox, P. de Rosnay, R. E. Dickinson, Y.-J. Dai, Q. Duan, J. Entin, P. Etchevers, N. Gedney, Y. M. Gusev, F. Habets, J. Kim, V. Koren, E. A. Kowalczyk, O. N. Nasonova, J. Noilhan, S. Schaake, A. B. Shmakin, T. G. Smirnova, D. Verseghy, P. Wetzel, Y. Xue, Z.-L. Yang, and Q. Zeng. The Representation of Snow in Land Surface Schemes: Results from PILPS 2(d). *Journal of Hydrometeorology*, 2:7–25, 2001.

S. Solomon, D. Qin, M. Manning, R. B. Alley, T. Berntsen, N. L. Bindoff, Z. Chen, A. Chidthaisong, J. M. Gregory, G. C. Hegerl, M. Heimann, B. Hewitson, B. J. Hoskins, F. Joos, J. Jouzel, V. Kattsov, U. Lohmann, T. Matsuno, M. Molina, N. Nicholls, J. Overpeck, G. Raga, V. Ramaswamy, J. Ren, M. Rusticucci, R. Somerville, T. F. Stocker, P. Whetton, R. A. Wood, and D. Wratt. Technical summary. in: Climate change 2007: The physical science basis. contribution of working group i to the fourth assessment report of the intergovernmental panel on climate change. Technical report, Cambridge University Press, Cambridge, United Kingdom and New York, NY, USA, 2007.

K. Stamnes, S. C. Tsay, W. Wiscombe, and K. Jayaweera. Numerically Stable Algorithm for Discrete-Ordinate Method Radiative Transfer in Multiple Scattering and Emitting Layered Media. *Applied Optics*, 27:2502–2510, 1988.

J. C. Stroeve, J. E. Box, and T. Haran. Evaluation of the MODIS (MOD10A1) Daily Snow Albedo Product over the Greenland Ice Sheet. *Remote Sensing of Environment*, 105:155–171, 2006.

D. Tanré, C. Deroo, P. Duhaut, M. Herman, J. J. Morcrette, J. Perbos, and P. Y. Deschamps. Descriptions of a Computer Code to Simulate the Satellite Signal in the Solar Spectrum: The S5 code. *International Journal of Remote Sensing*, 11(4):659–668, 1990.

E. F. Vermote and A. Vermeulen. Atmospheric Correction Algorithm: Spectral Reflectance (MOD09). MODIS Algorithm Technical Background Document NAS5-96062, NASA, 1999. Version 4.0.

D. L. Verseghy. CLASS - A Canadian Land Surface Scheme for GCMs. I. Soil model. *International Journal of Climatology*, 11:111–133, 1991.

D. Vikhamar. *Snow-Cover mapping in Forests by Optical Remote Sensing*. PhD thesis, Faculty of Mathematics and Natural Science, University of Oslo, Norway, 2003.

H. von Storch and F. W. Zwiers. *Statistical Analysis in Climate Research*. Cambridge University Press, 1999.

S. Wang, A. T. Trishchenko, K. V. Khlopenkov, and A. Davidson. Comparison of International Panel on Climate Change Fourth Assessment Report Climate Model Simulations of Surface

Albedo with Satellite Products over Northern Latitudes. *Journal of Geophysical Research*, 111(D21108), 2006.

S. G. Warren. Optical Properties of Snow. *Reviews of Geophysics and Space Physics*, 20(1): 67–89, 1982.

S. G. Warren and W. J. Wiscombe. A Model for the Spectral Albedo of Snow. II: Snow Containing Atmospheric Aerosols. *Journal of the Atmospheric Science*, 37:2724–2745, 1980.

S. G. Warren, V. F. Radinov, N. N. Bryazgin, Y. I. Aleksandrov, and R. Colony. Snow Depth on Arctic Sea Ice. *Journal of Climate*, 12:1814–1829, 1999.

J.-G. Winther, S. Gerland, J. B. Ørbæk, B. Ivanov, A. Blanco, and J. Boike. Spectral Reflectance of Melting Snow in a High Arctic Watershed on Svalbard: Some Implications for Optical Satellite Remote Sensing Studies. *Hydrological Processes*, 13:2033–2049, 1999.

J.-G. Winther, F. Godtliebsen, S. Gerland, and P. E. Isachsen. Surface Albedo in Ny-Ålesund, Svalbard: Variability and Trends During 1981-1997. *Global and Planetary Change*, 32:127–139, 2002.

W. J. Wiscombe and S. G. Warren. A Model for the Spectral Albedo of Snow. I: Pure Snow. *Journal of the Atmospheric Science*, 37:2712–2733, 1980.

Z.-L. Yang, R. E. Dickinson, A. Robock, and K. Y. Vinnikov. Validation of the Snow Submodel of the Biosphere-Atmosphere Transfer Scheme with Russian Snow Cover and Meteorological Observational Data. *Journal of Climate*, 10:353–373, 1997.